Biogeosciences, 22, 1887–1905, 2025
https://doi.org/10.5194/bg-22-1887-2025

Biogeosciences
Open Access

Effects of photosymbiosis and related processes on planktic foraminifera-bound nitrogen isotopes in South Atlantic sediments

Alexandra Auderset[1,2], **Sandi M. Smart**[3], **Yeongjun Ryu**[4], **Dario Marconi**[4], **Haojia Abby Ren**[5], **Lena Heins**[2], **Hubert Vonhof**[2], **Ralf Schiebel**[2], **Janne Repschläger**[2], **Daniel M. Sigman**[4], **Gerald H. Haug**[2], and **Alfredo Martínez-García**[2]

[1]School of Ocean and Earth Science, University of Southampton, Southampton, SO14 3ZH, UK
[2]Climate Geochemistry Department, Max Planck Institute for Chemistry Mainz, 55128 Mainz, Germany
[3]Department of Geological Sciences, University of Alabama, Tuscaloosa, AL 35401, USA
[4]Department of Geosciences, Princeton University, Princeton, NJ 08544, USA
[5]Department of Geosciences, National Taiwan University, Taipei, 106, Taiwan

Correspondence: Alexandra Auderset (a.auderset@soton.ac.uk)

Received: 21 July 2024 – Discussion started: 31 July 2024
Revised: 25 January 2025 – Accepted: 28 January 2025 – Published: 17 April 2025

Abstract. Foraminifera often form symbiotic relationships with photosynthetic algae, providing a host environment and inorganic nutrients in exchange for photosynthetic organic matter from the algal symbiont. To date, the history of this relationship has been studied in paleoceanographic records using the oxygen and carbon stable isotopes of foraminiferal calcite. More recently, photosymbiotic activity has been observed to impact the nitrogen isotope ratio (δ^{15}N) of foraminiferal tissue and the organic matter incorporated into foraminiferal tests. Dinoflagellate symbiont-bearing species appear to be lower in δ^{15}N than symbiont-barren species and more similar to their feeding sources, likely due to their retention of low-δ^{15}N metabolic ammonium and thus a weaker amplitude for the "trophic enrichment factor", the δ^{15}N increase per trophic level that is widely observed in food webs. We report new glacial–interglacial foraminifera-bound δ^{15}N (FB-δ^{15}N) data from Deep Sea Drilling Program Site 516, located in the subtropical South Atlantic gyre, which contains multiple foraminifera species at adequately high abundance for interspecies comparison of foraminiferal nitrogen, carbon, and oxygen isotopes over a full glacial cycle. Our data show a conserved δ^{15}N difference of 3 ‰–5 ‰ between dinoflagellate-bearing species and the other species, qualitatively consistent with, but greater in amplitude than, the δ^{15}N difference observed in previous modern ocean and core-top studies. We propose that this greater amplitude at Site 516 is the result of the lateral transport of symbiont-barren species into the South Atlantic subtropical gyre, which appears to represent a small region of low thermocline nitrate δ^{15}N surrounded by regions with higher thermocline nitrate δ^{15}N.

We demonstrate that FB-δ^{15}N provides a clear signal of dinoflagellate endosymbiosis and that it may be able to identify other, weaker endosymbioses (e.g., with chrysophytes or pelagophytes). However, the data also suggest caution in regions with strong gradients, where species from contrasting environments may occur in a single sediment sample.

1 Introduction

Biologically available nitrogen (or "fixed N") is an essential nutrient and thus central to ocean productivity and biogeochemical cycling (Sarmiento and Gruber, 2006), with links to atmospheric CO_2 and climate (Broecker, 1982; Broecker and Henderson, 1998; Falkowski, 1997; McElroy, 1983). The ocean's fixed N reservoir size is dominantly controlled by the balance between N_2 fixation and denitrification (Gruber and Sarmiento, 1997), which can be reconstructed by N isotopes (^{15}N/^{14}N, or δ^{15}N) measured on organic matter in marine sediments (Brandes and Devol, 2002; Deutsch et al., 2004; Galbraith et al., 2013). In addition, variation in the degree of nitrate consumption in ocean surface waters can also be investigated with N isotopes in marine sediments (Altabet and Francois, 1994).

Published by Copernicus Publications on behalf of the European Geosciences Union.

The isotopic composition of bulk N in marine sediments is variably influenced by diagenesis on the seabed and exogenous N inputs (e.g., Meckler et al., 2011; Robinson et al., 2012; Möbius, 2013; Schubert and Calvert, 2001). Largely to address these concerns, over the past decades, fossil-bound nitrogen isotope methods have been developed (Kast et al., 2022; Lueders-Dumont et al., 2018; Sigman et al., 1999; Wang et al., 2015; Wang et al., 2014; Brunelle et al., 2007; Robinson et al., 2004), including foraminifera-bound (FB-) δ^{15}N (Ren et al., 2009). In contrast to bulk sediment δ^{15}N, fossil-bound organic matter represents a specific N pool in the sediment archive that is physically protected from bacterial/chemical diagenesis, exogenous N contamination, and thermal stress by the biomineral matrix, and it appears to be minimally affected by partial calcite dissolution (Martínez-García et al., 2022). The first applications of the FB-δ^{15}N proxy focused on reconstructing past changes in the N cycle in the North Atlantic (Ren et al., 2009; Straub et al., 2013), Pacific (Ren et al., 2012a, 2017, 2015), and Southern Ocean (Martínez-García et al., 2014) over Pleistocene glacial–interglacial cycles. More recent studies have shown that FB-δ^{15}N can provide reliable information about changes in the N cycle through the Cenozoic (Auderset et al., 2022; Hess et al., 2023; Kast et al., 2019; Wang et al., 2022).

Studies in the oligotrophic ocean, where surface water nitrate is fully consumed, have established that FB-δ^{15}N in surface sediments reflects the δ^{15}N of shallow subsurface nitrate (i.e., the nitrate that is supplied to and consumed in the euphotic zone) (Ren et al., 2012b, 2009; Schiebel et al., 2018). Water column studies indicate seasonal changes in FB-δ^{15}N that parallel the changes in the δ^{15}N of bulk filtered particles ($> 0.7\,\mu$m) and/or net-tow-collected material ($> 150\,\mu$m) in surface waters (Smart et al., 2020, 2018), as is consistent with the role of planktic foraminifera as heterotrophic zooplankton that feed variously on phytoplankton, other heterotrophs, and other types of particulate N (PN) (e.g., Anderson et al., 1979; LeKieffre et al., 2020; Spindler et al., 1984; Takagi et al., 2019). Phytoplankton assimilate the nitrate supplied from below and provide the food to zooplankton such as foraminifera. The metabolism of zooplankton and other heterotrophs releases low-δ^{15}N regenerated N (e.g., ammonium), which is avidly reassimilated by phytoplankton. The net result is that phytoplankton biomass, on average, is lower in δ^{15}N than the nitrate supply (Altabet, 1988; Fawcett et al., 2011; Knapp et al., 2005), while herbivorous zooplankton are similar in δ^{15}N to the nitrate supply (Montoya et al., 2002). Foraminifera, which feed on both zooplankton and phytoplankton, thus have a δ^{15}N that varies with the δ^{15}N of the nitrate supplied and consumed in the euphotic zone (Ren et al., 2009, 2012b; Smart et al., 2018; Schiebel et al., 2018).

Aside from the δ^{15}N of their diet, some foraminifera species have a special aspect of their physiology that influences their δ^{15}N: most extant spinose planktic foraminifera species host algal symbionts (Hemleben et al., 1989). A typical heterotrophic organism puts most of its dietary organic carbon toward energy generation, releasing the metabolized carbon as CO_2. If the C : N : P of the organism is not vastly different from that of its food, this will leave the organism with an excess of N (as well as P). The N must be removed, typically being lost by deamination and excretion of the resulting ammonium (or of urea or uric acid that is produced from the ammonium). Foraminifera, like other symbiont-bearing organisms (e.g., scleractinian corals), take advantage of their metabolic N and P waste to obtain additional organic carbon: they provide these nutrients to symbiotic algae, which use them to fix additional organic carbon, with a portion of this organic matter then being returned to the host for its nutrition. This strategy is particularly prominent in low-nutrient marine systems, where environmental nutrient concentrations are low and light is abundant, such as in the oligotrophic subtropical gyres.

Because decisive steps in N catabolism break an N-containing bond, which involves substantial isotopic fractionation, the catabolically produced ammonium is low in δ^{15}N (Silfer et al., 1992). In normal heterotrophic organisms, the loss of this low-δ^{15}N ammonium raises the δ^{15}N of the organism, paraphrased by the isotope ecologist's rule of thumb: "You are what you eat plus a few (permille)" (DeNiro, 1976; DeNiro and Epstein, 1981). In dinoflagellate-bearing foraminifera, however, the dinoflagellates are thought to assimilate the low-δ^{15}N ammonium, recycling it back into the host–symbiont system and thus reducing the δ^{15}N elevation of the foraminifera relative to its food (Ren et al., 2009; Smart et al., 2018). In summary, because N excretion to the environment can be greatly reduced by photosynthetic endosymbiosis, foraminifera that host symbionts are expected to have a δ^{15}N closer to that of their food source and lower than "pure" heterotrophs with the same food source.

The role of symbiosis in ancient organisms and ecosystems is of great interest. In low- to midlatitude surface waters of the ocean, limitation of autotrophic biomass by the availability of nutrients (especially N and P) is common, and changes in ocean nutrient conditions through time may have played a major role in evolution (Hohmann-Marriott and Blankenship, 2011). Photosynthetic endosymbiosis – hosted by organisms such as scleractinian corals and planktic foraminifera – has been described as an adaptation to settings of N- and P-limited photosynthetic growth, with the heterotrophic host sharing its metabolic N and P with the autotrophic symbionts in exchange for organic carbon (C) (e.g., Hallock, 1981). Thus, the origin and history of these symbioses may reflect changes in the ocean's nutrient inventories and cycling. In turn, these symbioses may affect nutrient cycling and the availability of nutrients, especially in systems such as shallow reefs.

Photosymbiosis in modern foraminifera species can be investigated by microscopic observations of intracellular algae (Anderson and Be, 1976; Gastrich, 1987; Lee et al., 1965), pulse-chase experiments with isotope labels (Bird et al., 2020; LeKieffre et al., 2020), active chlorophyll fluorometry (Takagi et al., 2019), or detection of algal DNA (Gast and Caron, 1996; Gast et al., 2000). However, these methods may be complicated by foraminiferal feeding on algal cells, making it difficult to distinguish endosymbionts from prey. More to the point, identifying and/or quantifying photosymbiotic activity from fossil foraminifera is even more challenging, particularly for extinct species. The carbon isotopic composition (δ^{13}C) of the $CaCO_3$ of planktic foraminifera tests may be affected by photosymbiosis. Symbiotic photosynthetic organisms have a preference for taking up ^{12}C, resulting in local dissolved inorganic carbon (DIC) becoming enriched in ^{13}C, which is subsequently integrated into the calcium carbonate tests of foraminifera (Spero and DeNiro, 1987). In larger foraminifera specimens, which host a greater number of photosymbionts, there is a relatively higher enrichment of ^{13}C than in smaller individuals (Spero et al., 1991). Thus, the relationship between the δ^{13}C and test size of symbiont-bearing foraminifera has been proposed and applied as a metric by which to identify symbiosis in ancient foraminifera (D'Hondt et al., 1994; Edgar et al., 2013; Ezard et al., 2015; Norris, 1998). The oxygen isotopic composition (δ^{18}O) of the $CaCO_3$ can be used to infer the depth habitat of different foraminifera species, with higher δ^{18}O indicating deeper and colder water masses (e.g., Mulitza et al., 1997; Rashid and Boyle, 2007, and references therein). Thus, it has also been proposed that, due to persistent shallower depth habitats throughout the ontogeny of symbiont-bearing foraminifera, their size-specific δ^{18}O relationship should be minimal in comparison to symbiont-barren foraminifera species, which have a larger potential range of depth habitats (Rebotim et al., 2017). However, there are potential pitfalls to these approaches: the foraminiferal test size can be influenced by environmental conditions such as surface water stratification, with smaller test sizes reported during periods of upwelling (Schmidt et al., 2004). Furthermore, sediment mixing preferentially affects finer fractions and thus impacts the size fraction vs. δ^{13}C and δ^{18}O relationships (Hupp et al., 2019). Both proxies, their biological mechanisms, and their pitfalls require further investigation.

This study investigates foraminifera-bound nitrogen isotopes (FB-δ^{15}N) as a new tool for the reconstruction of past symbiosis in planktic foraminifera. We measure shell-bound δ^{15}N in five foraminifera species from a South Atlantic sediment core over a full glacial cycle. We also analyze the same samples for test δ^{18}O and δ^{13}C. In addition, in a subset of samples, we measure δ^{18}O and δ^{13}C in different test size fractions.

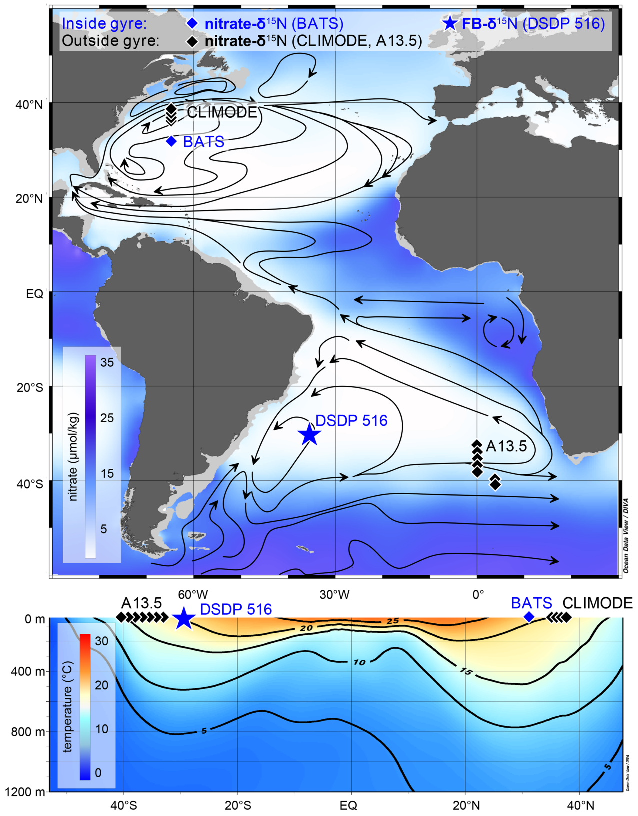

Figure 1. Oceanographic context for Deep Sea Drilling Program (DSDP) Site 516. **(a)** Nitrate map (in µmol kg^{-1}) at 100 m water depth with the sample location of DSDP Site 516 for FB-δ^{15}N (this study) and nitrate δ^{15}N profiles from CLIMODE (CLIvar MOde water Dynamics Experiment; this study), BATS (Fawcett et al., 2015), and A13.5 (this study). Main surface currents and oceanographic fronts modified from Peterson and Stramma (1991), Wefer et al. (1996), and Schmitz and McCartney (1993). **(b)** Mean annual temperature cross section. Map and cross section generated with Ocean Data View and the data set from the World Ocean Atlas (Garcia et al., 2014; Schlitzer, 2015).

2 Material and methods

2.1 Core site and local hydrography

We analyzed samples from sediment core DSDP (Deep Sea Drilling Program) Site 516, located on the Rio Grande Rise (30°16′ S, 35°17′ W; 1313 m water depth) near the core of the oligotrophic subtropical gyre in the South Atlantic Ocean (Fig. 1). The local hydrography is dominated by the wind-driven anticyclonic South Atlantic gyre. The subtropical gyre is associated with net subduction, deepened isopycnals, slow nutrient supply from the subsurface to the euphotic zone, and N and P impoverishment in the euphotic zone (Cullen et al., 2002). The nutrient supply to the euphotic zone at Site 516 can be augmented by eddy mixing with the nutrient-bearing waters of the Antarctic Circumpolar Current, which flow east-northeastward along the southern boundary of the gyre (Reid et al., 1977; Schmid et al., 2000). The Brazil Current to the west may also contribute nutrients. However, Site 516 is near the core of the gyre and is relatively isolated from nutrient inputs at the margins. Accordingly, the annual average nitrate concentration ranges from 0.2 $\mu mol\,kg^{-1}$ to below the limit of detection, and chlorophyll *a* concentrations are $< 0.7\,mg\,m^{-3}$ (Siccha et al., 2018). These conditions are comparable to those observed in the oligotrophic Sargasso Sea in the North Atlantic, as established for the Bermuda Atlantic Time-series Study (Lomas et al., 2013; Steinberg et al., 2001). The eastern boundary of the subtropical gyre is marked by the Benguela Current, where the persistent southerly and southeasterly winds drive surface water offshore and facilitate the upwelling of cold and nutrient-rich subsurface water (Cole and Villacastin, 2000). The Benguela Current flows northward and turns into the southern branch of the South Equatorial Current, which forms the northern edge of the subtropical gyre (Stramma, 1991).

2.2 Nitrogen isotope analysis

2.2.1 Foraminifer-bound nitrogen isotopes

Sediment samples were wet sieved through a 63 µm mesh and dried overnight in a clean oven at 40 °C. Between 600 and 800 individual foraminifera tests were manually picked from the 250–400 µm size fraction. We analyzed dinoflagellate-bearing *Trilobatus sacculifer*, the two chromotypes *Globigerionoides ruber ruber* and *G. ruber albus* (pink and white, respectively), chrysophyte-bearing *Globigerinella siphonifera* (synonym *G. aequilateralis*), and symbiont-barren *Globigerina bulloides* and *Globorotalia truncatulinoides*. The detailed protocol used here for measuring FB-δ^{15}N can be found in Auderset et al. (2022) and Moretti et al. (2024). In short, about 5–7 mg of foraminifera tests were gently crushed and chemically treated to remove external organic matter, clay, and manganese coatings. Subsequently, 3–5 mg of the cleaned material was weighed out per sample for N content determination and, ultimately, N isotope analysis. The test fragments were first dissolved in hydrochloric acid (50 µL of 3N HCl), and the organic N was converted into nitrate (NO_3^-) by persulfate oxidation following a slightly modified protocol first used for foraminifera by Ren et al. (2009). The NO_3^- was converted to nitrous oxide (N_2O) using denitrifying bacteria *Pseudomonas chlororaphis*, and its δ^{15}N was measured by an automated, custom-built N_2O extraction system and inlet by continuous helium carrier flow to an isotope ratio mass spectrometer (Thermo MAT 253) (Casciotti et al., 2002; Sigman et al., 2001; Weigand et al., 2016). To quantify the precision and accuracy of the corrected isotope values, for each series of 30 samples, a total of three different in-house (Max Planck Institute for Chemistry – MPIC) calcite and aragonite laboratory standards were analyzed in triplicate, namely a coral standard from the taxon *Porites* (PO-1) with δ^{15}N of 6.2 ± 0.3 ‰, a coral standard from the taxon *Lophelia* (LO-1) with δ^{15}N of 10.1 ± 0.4 ‰, and a mixed foraminifera standard (MF-1) (63–315 µm size fraction) from the North Atlantic (MSM58-17-1; Repschläger et al., 2018) with δ^{15}N of 5.92 ± 0.28 ‰ (Moretti et al., 2024). After correcting for blank isotope composition, the precision of the multi-analysis average from each run is better than 0.2 ‰ (± 1 SD).

2.2.2 Seawater nitrate nitrogen isotopes

Seawater samples from the South Atlantic A13.5 section were collected from full-water-column hydrocasts, spanning 32.0 to 41.5° S. Acid-washed 60 mL high-density polyethylene bottles (Nalgene) were rinsed at least three times with sample water prior to filling and immediately frozen at −20 °C until analysis for NO_3^- concentration and δ^{15}N. For comparison, we also measured seawater from the upper 1000 m of the water column in the subtropical North Atlantic gyre, collected during the CLIMODE (CLIvar MOde water Dynamics Experiment) campaign in 2006 (Hutto et al., 2006). Sampling stations are located across the northern boundary of the subtropical gyre between roughly 36.45 and 38.6° N, which covers the sharp transition in water properties associated with the northern edge of the subtropical gyre (Fig. 1).

As with FB-δ^{15}N analysis, the δ^{15}N (vs. air) and δ^{18}O (vs. Vienna Standard Mean Ocean Water – VSMOW) of NO_3^- were determined using the denitrifier method (Casciotti et al., 2002; Sigman et al., 2001). For seawater, denitrifying bacteria *Pseudomonas chlororaphis* ssp. *aureofaciens* (ATCC 13985, Manassas, VA, USA) were used to quantitatively convert the NO_3^- and nitrite (NO_2^-) in samples to N_2O. The product N_2O was analyzed as described above (Weigand et al., 2016). For the shallow-water samples, where NO_2^- constitutes over 10 % of the total $NO_2^- + NO_3^-$ pool, mostly in the upper 200 m, sulfamic acid was added to remove NO_2^- following the protocol described by Granger and Sigman (2009). The pooled standard deviation of all NO_3^--only and $NO_2^- + NO_3^-$ δ^{15}N measurements, respectively, were 0.24 ‰ (for shallow samples, < 200 m) and 0.08 ‰ (for deeper samples). Two international potassium nitrate (KNO_3) reference materials, IAEA-N3 (δ^{15}N of 4.7‰, δ^{18}O of 25.6‰) and USGS-34 (δ^{15}N of −1.8 ‰, δ^{18}O of −27.9‰), were used for standardization, and a lab N_2O standard in helium was run in parallel to monitor the consistency of mass spectrometry.

2.3 Stable oxygen and carbon isotope analysis

For the down-core records of δ^{18}O and δ^{13}C, we picked samples of all five species from the 250–400 µm size fraction throughout the core. For reference, the largest test sizes for *T. sacculifer* and *G. siphonifera* were observed in the 400–630 µm size fraction, whereas the largest test sizes for *G. truncatulinoides* were found in the > 630 µm size fraction. To investigate the size-fraction-specific δ^{13}C and δ^{18}O, we chose specimens with sizes of 200–250, 250–315, 315–400, and > 400 µm from two climatically distinct (end-member) settings: an interglacial (129 ka; Marine Isotope Stage (MIS) 5) and glacial (27 ka; Last Glacial Maximum (LGM)) time period. There were not enough *G. bulloides* tests within the two largest size fractions (315–400 and > 400 µm); thus, size-specific δ^{13}C and δ^{18}O could not be evaluated for this species. For each sample measured, 30 specimens were gently cracked open with a watch glass, submerged in aliquots of ethanol (pure grade), and put in an ultrasonic bath for 20 s. Subsequently, the ethanol was decanted and the samples were dried at 60 °C in a clean oven. Clean sample fragments were placed in 4.5 mL Exetainer vials, flushed with helium, and digested by anhydrous orthophosphoric acid (H_3PO_4) at 70 °C. The liberated CO_2–He mixture was transported to the Thermo Finnigan GasBench II preparation device with He as the carrier gas and analyzed using a Thermo Finnigan DELTA V mass spectrometer (Breitenbach and Bernasconi, 2011). For each series of 60 samples, four different calcite laboratory standards were analyzed in quintuplicate. $CaCO_3$ standard weights were chosen so that they spanned the entire range of sample weights. VU Internal Carbonate Standards (VICS) were used to correct for sample-size-based fractionation effects. VICS, International Atomic Energy Agency (IAEA) standards, and two in-house carbonate standards (travertine and Carrara marble) were used to detect mass spectrometer drift during the run and to quantify the precision and accuracy of the corrected isotope data. After correction for these effects, the reproducibility of the standards was typically better than 0.1 ‰ (± 1 SD) for both δ^{18}O and δ^{13}C.

2.4 Age model

The age model for DSDP 516 was produced by graphically aligning benthic foraminifera oxygen isotopes (Auderset et al., 2024) with global benthic stack LR04 by Lisiecki and Raymo (2005) using the AnalySeries software (Paillard et al., 1996).

3 Results

Down-core changes in FB-δ^{15}N and δ^{13}C are small relative to interspecies differences. The weak changes in δ^{15}N across the last 160 kyr are discussed elsewhere (Auderset et al., 2024). Here, we focus on the interspecies differences (Figs. 2, 3). FB-δ^{15}N data show two distinct groups: *T. sacculifer*, *G. ruber albus*, and *G. ruber ruber* of ca. 4.2 ‰ (±0.42), 4.1 ‰ (±0.43), and 4.3 ‰ (±0.37), respectively, vs. *G. truncatulinoides*, *G. bulloides*, and *G. siphonifera*, which show more elevated δ^{15}N values of 8.0 ‰ (±0.67), 9.3 ‰ (±0.45), and 8.8 ‰ (±0.46), respectively (Figs. 2a, 3a). The N contents range between 3.8 and 4.5 nmol mg^{-1} (Figs. 2b, 3b). We observe similar N contents throughout the record and among the species. The studied foraminifera are well preserved, and the stability of the N content through the record implies little to no diagenetic loss of FB-N after burial through the sediment mixed layer (Fig. S1).

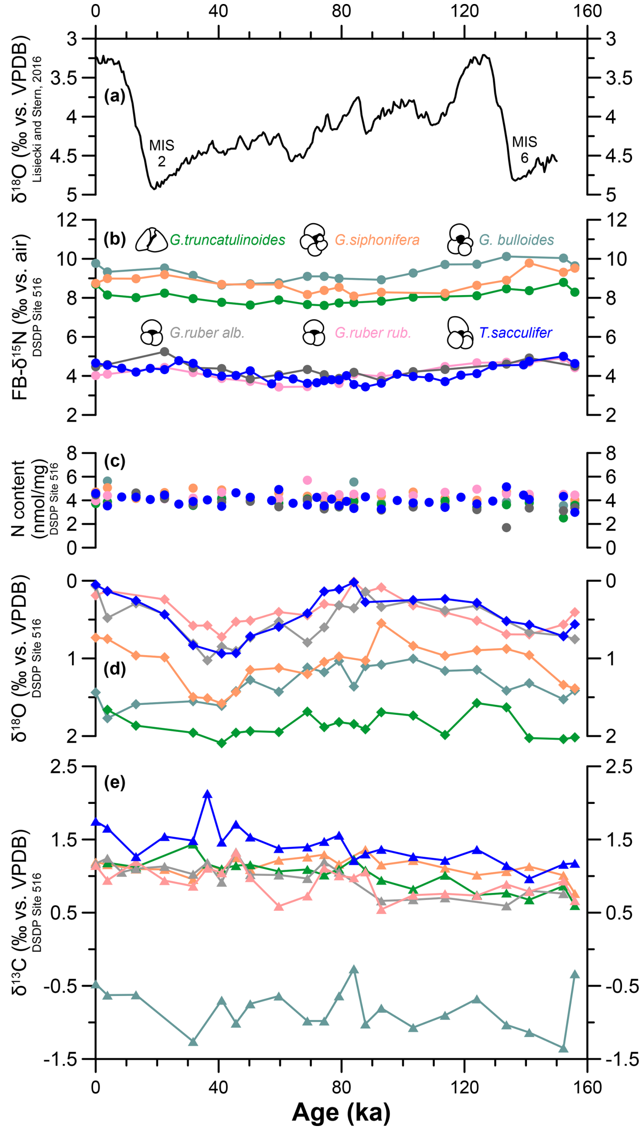

Figure 2. The 160 kyr time series of species-specific nitrogen, carbon, and oxygen isotopes at DSDP Site 516. **(a)** Benthic foraminifera δ^{18}O stack (Lisiecki and Stern, 2016). MIS denotes Marine Isotope Stage. **(b)** Species-specific FB-δ^{15}N measured at DSDP 516 for *G. bulloides* (turquoise), *G. siphonifera* (orange), *G. truncatulinoides* (green), *T. sacculifer* (blue), *G. ruber ruber* (pink), and *G. ruber albus* (gray). **(c)** N content for each species. **(d)** Species-specific calcite-δ^{18}O and **(d)** calcite-δ^{13}C.

The δ^{18}O data show a fairly even spread between the different species (Figs. 2c, 3c). *Trilobatus sacculifer* and *G. ruber* (*albus* and *ruber*) are more depleted in ^{18}O (with δ^{18}O values of 0.3 ‰–0.5 ‰) compared with *G. truncat-*

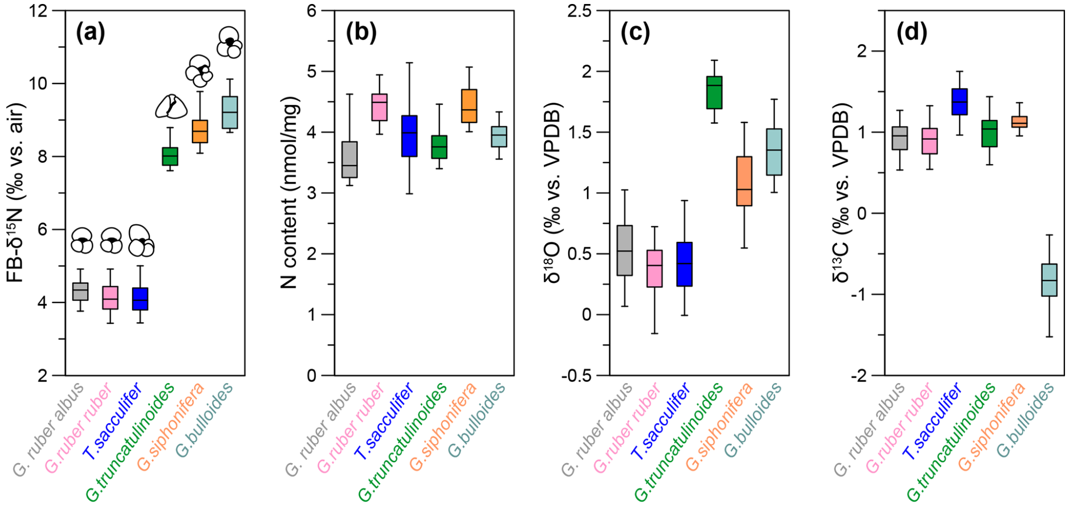

Figure 3. Box plots of species-specific nitrogen, carbon, and oxygen isotopes at DSDP Site 516. **(a)** Species-specific FB-δ^{15}N values averaged over the last 160 kyr for *G. bulloides* (turquoise), *G. siphonifera* (orange), *G. truncatulinoides* (green), *T. sacculifer* (blue), *G. ruber ruber* (pink), and *G. ruber albus* (gray). **(b)** N content for each species. Panels **(c)** and **(d)** present the species-specific δ^{18}O and δ^{13}C, respectively.

ulinoides, *G. bulloides*, and *G. siphonifera* (1.1 ‰–1.9 ‰). Over the last 160 kyr, *T. sacculifer*, *G. ruber* (*albus* and *ruber*), and *G. siphonifera* generally follow the same trend. These species show a temporal variation of ∼ 0.7 ‰–1 ‰ with a maximum at 40 ka and minimum at 90 ka (Figs. 2c, 3c). *Globorotalia truncatulinoides* and *G. bulloides* show a smaller amplitude of variation of ∼ 0.5 ‰ and no clear δ^{18}O maximum/minimum (Figs. 2c, 3c). Apart from *G. bulloides* with a δ^{13}C range between −1.6 ‰ and −0.3 ‰, all species range between 0.6 ‰ and 1.7 ‰. *Globigerina bulloides* δ^{13}C shows a substantial negative offset of ca. 1.5 ‰ from the other species and is more variable than all of the other species analyzed here (Figs. 2d, 3d).

All species investigated appear to show a positive relationship between test carbonate δ^{13}C and test size, although some reversals occur in the largest (400 µm) size fraction (data for *G. bulloides* are for the two smallest size fractions only) (Fig. S2). We record different slopes of the linear fit in LGM and MIS 5 samples (the two end-member settings) for *T. sacculifer* and *G. ruber* (*albus* and *ruber*) (Table S1). The Pearson correlation coefficient (r value) for the LGM ranges between 0.60 and 0.98, whereas it is between 0.68 and 0.96 for MIS 5, with *G. siphonifera* and *G. truncatulinoides* having the lowest r values among the studied species. The slopes for δ^{13}C vs. test size remain relatively constant for *G. siphonifera* (0.0013 vs. 0.0024) and *G. truncatulinoides* (0.0043 vs. 0.0038) between the LGM and MIS 5. However, the strength of the relationship differs between the two intervals, with r values for *G. siphonifera* increasing from 0.60 during the LGM to 0.86 in MIS 5, and values for *G. truncatulinoides* decreasing from 0.91 to 0.68 during the same period. *T. sacculifer* exhibits the highest average slope for both time slices (0.053), while *G. siphonifera* records the lowest (0.018). Notably, significant relationships ($p < 0.05$) for δ^{13}C are observed in *G. ruber albus* ($p = 0.02$) and *G. ruber ruber* ($p = 0.03$) during the LGM and in *T. sacculifer* ($p = 0.04$) during MIS 5.

In contrast to δ^{13}C, the test carbonate δ^{18}O shows only a weak correlation with test size (Table S1), and the relationship varies down the core and between species (Fig. S3). The only significant relationship is observed for *G. ruber albus* in the combined time slice ($p = 0.02$).

Seawater nitrate nitrogen isotopes and nitrate concentration profiles from CLIMODE and A13.5 stations are shown in Fig. S4 and discussed in the Supplement.

4 Discussion

4.1 FB-δ^{15}N at DSDP Site 516

In the planktic foraminifera species *T. sacculifer* and *G. ruber*, dinoflagellate symbionts may recycle low-δ^{15}N ammonium and thus keep FB-δ^{15}N low, preventing the full ca. 3 ‰ elevation characteristic of a trophic level increase (Minagawa and Wada, 1984; Ren et al., 2012b; Smart et al., 2018). Therefore, the δ^{15}N of *T. sacculifer* and *G. ruber* should more closely match the δ^{15}N of their food source than in species without dinoflagellate symbionts. In oligotrophic areas, such as the subtropical South Atlantic gyre, surface nitrate is fully consumed by phytoplankton. With the role of euphotic zone N recycling described in Sect. 1 (Altabet, 1988; Fawcett et al., 2011), this leads to herbivorous zooplankton close to or slightly higher than the δ^{15}N of this consumed nitrate, e.g., 3.6 ± 1.0 ‰ ($n = 107$) for zooplankton vs. 2.6 ‰ for thermocline nitrate in the Sargasso Sea (Montoya et al., 2002; Smart et al., 2018). With foraminifera feeding on a mixture of small and large phytoplankton and zooplankton, this yields a δ^{15}N for the foraminifera diet that is close to the δ^{15}N of the subsurface nitrate supply (Fawcett et al., 2011). At DSDP Site 516, the FB-δ^{15}N of the dinoflagellate-bearing species *T. sacculifer* and *G. ruber* (Gastrich, 1987; Hemleben et al., 1989) ranges between 4 ‰ and 5 ‰. This value is lower than global mean pycnocline nitrate (of 6.25 ‰; Fripiat et al., 2021), suggesting that regional subsurface nitrate δ^{15}N has been lowered by N_2 fixation, as has been observed in other subtropical gyres (Harms et al., 2019; Knapp et al., 2008; Marshall et al., 2022; Casciotti et al., 2008; Liu et al., 1996; Yoshikawa et al., 2015), especially the North Atlantic (Marconi et al., 2015, 2017). For comparison, in the Sargasso Sea – an ocean region with persistent N_2 fixation – shallow thermocline nitrate δ^{15}N is 2.6 ‰ (Fawcett et al., 2015) and surface sediment FB-δ^{15}N values are 2.4 ‰ (*T. sacculifer*) and 2.6 ‰ (*G. ruber*) (Smart et al., 2018).

In *G. truncatulinoides*, the bulk of the shell derives from calcification below 100 m, indicating that they spend much of their lives below the euphotic zone, where light conditions are unsuitable for photosymbionts (Reynolds et al., 2018; Schiebel and Hemleben, 2017). This is consistent with their high δ^{15}N compared with dinoflagellate symbiont bearers. *G. bulloides* and *G. siphonifera* are more enriched in ^{15}N than the other analyzed species at DSDP Site 516. This may indicate minimal nitrogen recycling associated with non-dinoflagellate symbionts, e.g., chrysophytes for *G. siphonifera*, such that this species groups with the symbiont-barren species (Faber et al., 1989, 1988; Ren et al., 2012b; Smart et al., 2018; Granger et al., 2024). As for the higher δ^{15}N of *G. bulloides* and *G. siphonifera* relative to *G. truncatulinoides,* this might be explained by a higher δ^{15}N for their food source. This possibility is pursued in Sect. 4.4.

4.2 Comparison with carbonate oxygen and carbon isotopes at DSDP Site 516

To gain additional insight into the controls on FB-δ^{15}N, we compare the data with our measurements of carbonate δ^{18}O and δ^{13}C of the foraminiferal shells. The δ^{18}O differences among species have been used to reconstruct depth habitat (Fairbanks and Wiebe, 1980; Ravelo and Fairbanks, 1980). Minimum δ^{18}O values in foraminiferal assemblages point to warmer waters and shallower depth habitats, which are likely to be required or at least best-suited for photosymbiont-bearing foraminifera (Fig. 4a) (see also the Supplement). By cross-plotting FB-δ^{15}N and δ^{18}O from Site 516, we see two distinct groups: (1) shallow dwellers with dinoflagellate symbionts with lighter FB-δ^{15}N and δ^{18}O and (2) deeper dwellers with non-dinoflagellate symbionts/symbiont-barren species recording heavier FB-δ^{15}N and δ^{18}O (Fig. 4b). Thus, unsurprisingly, the measurements are consistent with a shallow depth habitat for photosymbiosis.

The controls on the δ^{13}C of planktic foraminiferal calcite are a matter of debate (Spero and Williams, 1989; Spero et al., 1991); however, size-specific δ^{13}C measurements have been proposed as a proxy for photosymbiosis. Foraminiferal δ^{13}C is likely sensitive to both environmental- and organism-scale δ^{13}C gradients (induced by photosymbiont activity and foraminifera respiration), with a ^{13}C enrichment for increased photosynthetic activity (Spero et al., 1997; Spero and DeNiro, 1987). However, the δ^{13}C of the deepest dwelling, symbiont-barren species *G. truncatulinoides* at DSDP Site 516 does not distinguish it from even the most photosymbiotically active species (Figs. 2d, 3d). This is because depth habitat, variation in dissolved inorganic carbon, remineralization, and other environmental factors also influence carbonate δ^{13}C, such that it alone is unlikely to be a reliable proxy for photosymbiosis. Surface mixed-layer DIC is typically enriched in ^{13}C due to photosynthesis, whereas subsurface water DIC δ^{13}C is lower due to bacterial respiration and remineralization of the low-δ^{13}C organic matter arriving from the euphotic zone (Kroopnick, 1985). In a stratified ocean, such as the South Atlantic subtropical gyre, shallow-dwelling foraminifera should thus incorporate a higher δ^{13}C in contrast to thermocline dwellers with lower δ^{13}C. However, at DSDP Site 516, modern surface ocean $\delta^{13}C_{DIC}$ seems to be only marginally higher ($\sim$ 1.7 ‰) than the $\delta^{13}C_{DIC}$ in the upper thermocline ($\sim$ 1.4 ‰) (Fig. S7), which could explain why the calcite δ^{13}C values of *T. sacculifer* and *G. truncatulinoides* at Site 516 are so similar. In our measurements, the shallow subsurface/thermocline dweller *G. bulloides* is the only species to be clearly lower in δ^{13}C than the other foraminifera. It has been speculated that the presence of metabolically active cyanobacterial endobionts (*Synechococcus*) affects the carbon isotopes measured in the host *G. bulloides* through respiration, instead of photosynthesis from the endobiont, leading to ^{13}C depletion instead of ^{13}C enrichment in the calcifying microenvironment (Bird et al., 2017; Febvre-Chevalier, 1971; Spero and Lea, 1996). Alternatively, we suspect that this offset could be due to other effects associated with seasonality (Sect. 4.4.2) or a different environmental baseline for foraminifera originating from outside the South Atlantic gyre (Sect. 4.4.3).

In any case, the cross-plot between FB-δ^{15}N and δ^{13}C strongly discriminates between *G. bulloides* vs. the other foraminifera analyzed at Site 516 (Fig. 4c). Interestingly, *G. siphonifera* clusters in the same group as *G. truncatulinoides*, although both species are very different in terms of depth habitat and symbiotic relationship. Altogether, the δ^{15}N–δ^{13}C comparison might be interpreted as indicating that the non-dinoflagellate symbionts have a significant but variable effect on carbonate δ^{13}C while having no appreciable effect on FB-δ^{15}N (Fig. 4c). However, this view is complicated for δ^{13}C by the observation that *G. truncatulinoides*, which is a symbiont-barren species, has a similar δ^{13}C to species with a range of symbionts.

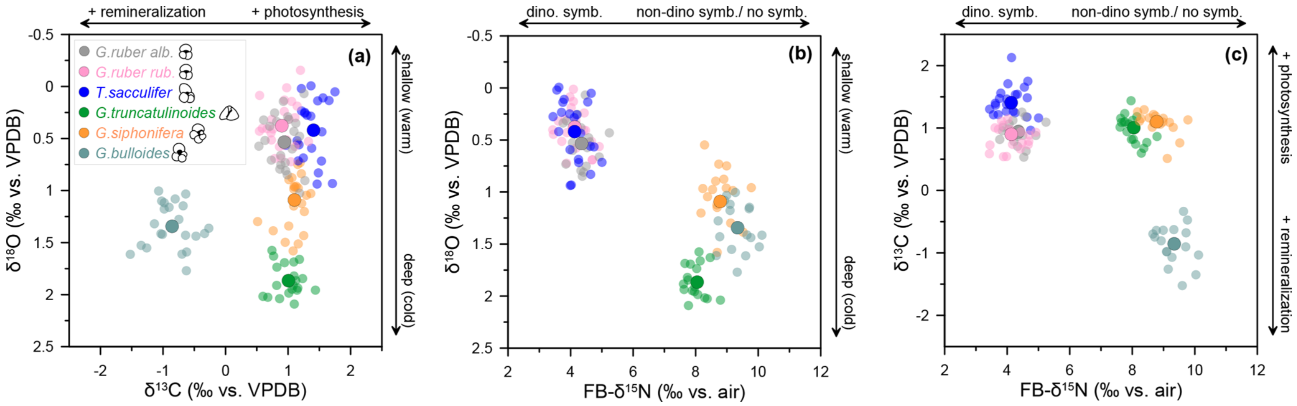

Figure 4. Relationships between oxygen, carbon, and nitrogen isotopes. Interspecies comparison between *G. ruber* (*albus* and *ruber*), *T. sacculifer, G. truncatulinoides*, *G. siphonifera*, and *G. bulloides* at DSDP Site 516. Arrows indicate the distinction between shallow (warm) vs. deep (cold) dweller, remineralization vs. photosynthesis in the water column, and non-dinoflagellate-bearing/non-symbiotic vs. dinoflagellate-bearing foraminifera.

An alternative method proposed for the detection of photosymbiosis in fossil foraminifera is through the relationship of foraminiferal carbonate δ^{13}C with test size (Spero and DeNiro, 1987). The argument is that the preferential uptake of $^{12}CO_2$ by the photosynthesizing symbionts raises the δ^{13}C of the internal DIC pool from which the calcification proceeds (Spero et al., 1997). Larger individual foraminifera can host more symbionts per surface area of the individual, resulting in δ^{13}C elevation compared with smaller foraminifera (Spero et al., 1991). Thus, a steeper rise in δ^{13}C with increasing specimen size (steeper positive slope) indicates potentially higher photosymbiotic activity (Edgar et al., 2013; Norris, 1996; Shaw et al., 2021). According to this method, dinoflagellate-bearing *G. ruber* and *T. sacculifer* and potentially chrysophyte-hosting *G. siphonifera* would be predicted to have a steeper rise in δ^{13}C with size than *G. truncatulinoides* or *G. bulloides*. However, for all investigated species except *G. siphonifera*, our measurements indicate similar slopes in δ^{13}C vs. size, with dinoflagellate-bearing species *T. sacculifer*, and *G. ruber* (*albus* and *ruber*) showing no statistically significant difference in slopes compared to the non-symbiotic species *G. truncatulinoides* (Fig. S2, Table S1). The weak/near-zero slope for *G. siphonifera* δ^{13}C (Fig. S2e) could be the result of the size fraction between 125 and 400 µm used in this study not capturing the larger, adult life stages of this species; we also observed a small number of *G. siphonifera* in the 400–630 µm fraction but did not measure them. Nevertheless, the anomalously weak/near-zero slope for *G. siphonifera* δ^{13}C has been observed before. Bijma et al. (1998) showed a steeper slope for *G. siphonifera* type II than type I. They proposed that *G. siphonifera* type-I symbionts are less efficient at removing low-δ^{13}C host-respired CO_2, allowing respiration to partially counteract the photosynthesis-induced δ^{13}C rise in the microenvironment and shells during ontogeny. The significant contribution of host-respired CO_2 to symbionts in *G. siphonifera* type II is supported by the recent experimental study by Takagi et al. (2022).

That *G. truncatulinoides* falls into the same range of slopes (as well as absolute δ^{13}C values) as *T. sacculifer* and *G. ruber* and has a steeper slope than *G. siphonifera* indicates that either the size fraction was too low and we observe the difference between juveniles and adults in *G. truncatulinoides* or that the previously proposed symbiosis metric of δ^{13}C vs. size may not be sensitive enough to capture all photosymbiotic relationships.

However, using FB-δ^{15}N as a symbiosis proxy may also have its complexities. In particular, the FB-δ^{15}N differences between foraminifera with and without dinoflagellate symbionts is notably greater at DSDP Site 516 than reported at other sites across the global ocean (Costa et al., 2016; Martínez-García et al., 2014; Ren et al., 2012b; Schiebel et al., 2018; Smart et al., 2020, 2018). Interspecies FB-δ^{15}N relationships might vary due to processes in the water column, such as seasonal changes in the supply of N affecting the δ^{15}N of the food source (Smart et al., 2020, 2018) or lateral transport (Granger et al., 2024). In the next section, we compare DSDP Site 516 with core-top samples from geographically distinct regions to examine the variability in FB-δ^{15}N differences amongst foraminifera species relative to the oceanographic environment.

4.3 FB-δ^{15}N as a new proxy for photosymbiosis?

To further advance our understanding of FB-δ^{15}N and its suitability as a metric of photosymbiosis, we now broaden our view beyond DSDP Site 516. We compile all available and published core-top FB-δ^{15}N data that contain dinoflagellate-bearing and non-dinoflagellate-bearing foraminifera (Fig. S5, Table S2). The calculated offsets between the two categories across all core sites show that non-dinoflagellate-bearing foraminifera (*Globorotalia menardii*,

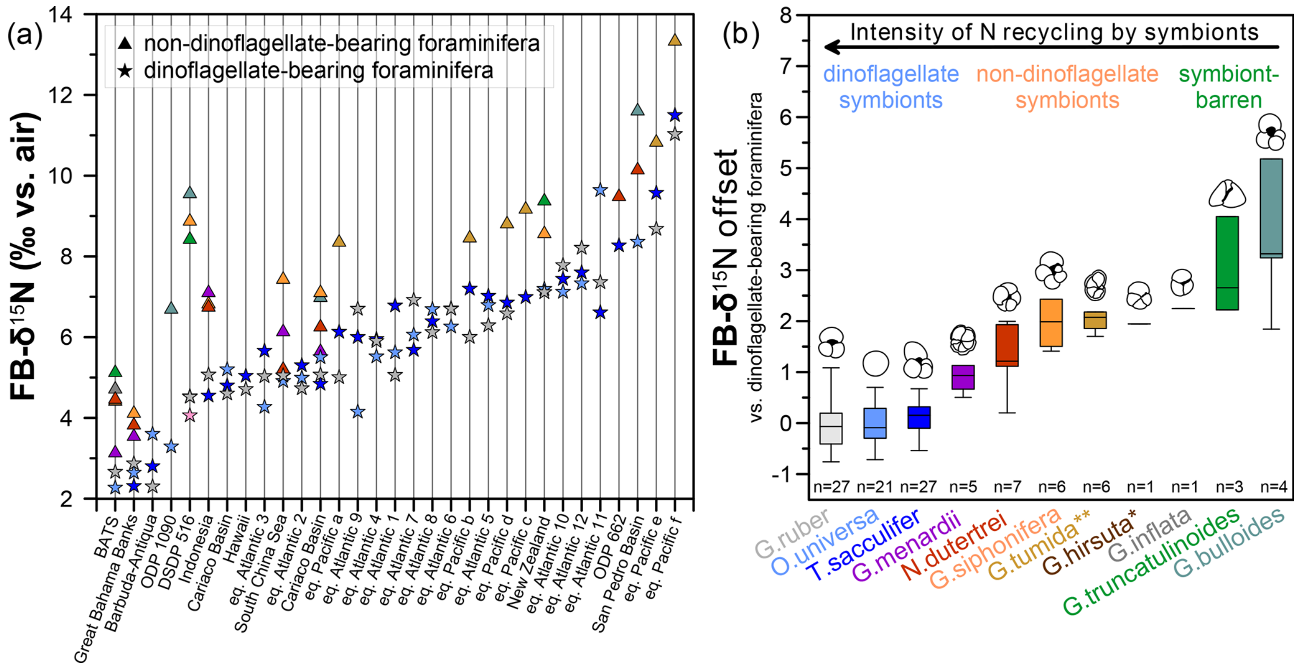

Figure 5. Compilation of FB-δ^{15}N values and offsets between dinoflagellate-bearing and non-dinoflagellate-bearing foraminifera from different locations. **(a)** Foraminifera from core tops in the Sargasso Sea (BATS) (Smart et al., 2018), Great Bahama Banks, Indonesia, Hawaii, South China Sea, Aotearoa / New Zealand (Ren et al., 2012b), and equatorial Atlantic 1–12 (Schiebel et al., 2018) as well as Holocene samples from the equatorial Pacific a–f (Costa et al., 2016), Ocean Drilling Program (ODP) Site 1090 (Martínez-García et al., 2014), ODP Site 662 (Auderset et al., 2024) and DSDP Site 516 (this study) (see Table S2 and Fig. S5 for more information about core sites). **(b)** Across all sites in panel **(a)**, the average FB-δ^{15}N offset between and dinoflagellate-barren and dinoflagellate-bearing foraminifera is categorized by symbiont relationship and proposed intensity of internal ammonium recycling. An asterisk (*) denotes suspected chrysophyte symbiont-bearing or symbiont-barren species, whereas two asterisks (**) denote an unknown symbiotic status.

Neogloboquadrina dutertrei, *G. siphonifera*, *Globorotalia tumida*, *Globorotalia hirsuta*, *Globorotalia inflata*, *G. truncatulinoides*, and *G. bulloides*) are consistently enriched in ^{15}N compared with dinoflagellate-bearing foraminifera (*G. ruber*, *T. sacculifer*, and *O. universa*) (Fig. 5a). For the most part, FB-δ^{15}N offsets are consistent across wide geographic ranges of the core sites over different latitudes and biogeochemical regimes. With this compilation, we first consider the average FB-δ^{15}N values that arise for different species and their implications for FB-δ^{15}N differences among different symbioses (Figs. 5b, 6).

The calculated mean FB-δ^{15}N offsets between dinoflagellate bearing and non-dinoflagellate/symbiont-barren foraminifera from the global compilation correlate with chlorophyll *a* (Chl *a*) measurements by Takagi et al. (2019). They analyzed living foraminifera from the central and western Pacific Ocean and the tropical eastern Atlantic Ocean across different seasons and estimated the intensity of photosymbiosis (Fig. 7). Based on Takagi et al. (2019), *O. universa*, *T. sacculifer*, *G. ruber ruber*, and *G. ruber albus* have a higher percentage of intracellular Chl *a* and thus photosymbiont activity. This is in contrast to *G. truncatulinoides*, *G. bulloides*, and *G. inflata*, with little/no Chl *a* inside of the tests, which record the highest FB-δ^{15}N compared with dinoflagellate-bearing foraminifera (*G. ruber*, *T. sacculifer*, and *O. universa*) (Fig. 5b). *Neogloboquadrina dutertrei* and *G. menardii* are consistently higher in Chl *a*/biomass and lower with respect to their FB-δ^{15}N offset than photosymbiont-barren *G. bulloides* and *G. truncatulinoides*. However, the strength of the Chl *a*/biomass vs. FB-δ^{15}N relationship is not extraordinarily strong ($r = 0.72$), suggesting that the Chl *a* content is not the only factor driving FB-δ^{15}N (Fig. 7).

Globigerinella siphonifera stands out in the correlation of Chl *a*/biomass in the global compilation (Fig. 7), as it records similar levels of Chl *a*/biomass compared with some dinoflagellate symbiont-bearing foraminifera *G. ruber* (*ruber* and *albus*), despite their high FB-δ^{15}N offset from dinoflagellate-hosting foraminifera reported at DSDP Site 516 (Fig. 3a) and in previous studies (Li et al., 2019; Ren et al., 2012b; Smart et al., 2018; Granger et al., 2024). Takagi et al. (2016) find that the chlorophyll content of *G. siphonifera* peaks before the final chamber formation, resulting in a minimum chlorophyll content during formation of the largest–second-largest chamber, which likely dominate calcite mass (and thus geochemistry). This may reflect digestion of its symbionts prior to gametogenesis (Faber et al., 1988), making *G. siphonifera* a symbiont-barren species in its later

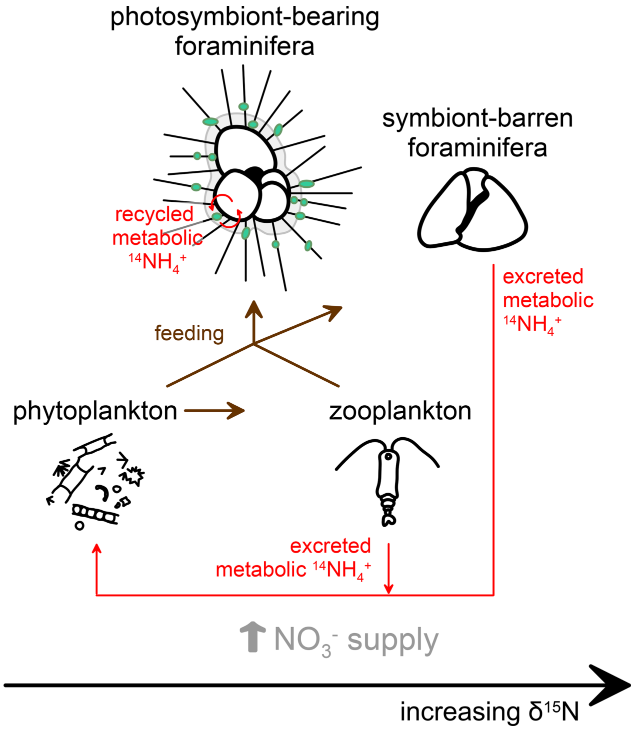

Figure 6. Proposed interactions and processes influencing planktic foraminifera-bound nitrogen isotopes (FB-δ^{15}N) in relation to symbiotic status and food sources. Symbiont-barren foraminifera or those hosting symbionts other than dinoflagellates record elevated FB-δ^{15}N relative to their food source, as with typical zooplankton. In contrast, symbiont-bearing foraminifera exhibit lower FB-δ^{15}N values due to their association with photosymbionts, which internally reassimilate the low-δ^{15}N metabolic ammonium (NH_4^+) from the foraminiferal host in their photosynthetic growth, preventing or reducing the δ^{15}N elevation that typically results from heterotrophy.

stages of calcification. In any case, this ontogenetic change could explain why FB-δ^{15}N would identify *G. siphonifera* as having a weaker host–symbiont N cycle. As an alternative or additional explanation, the high FB-δ^{15}N and relatively high Chl *a* of *G. siphonifera* may indicate a less active symbiotic relationship, whether due to less efficient internal ammonium recycling (Smart et al., 2018), low chrysophyte growth rates, and/or higher harvesting rates.

All such interpretations, however, are currently uncertain. Across species of foraminifera, symbiont physiology, photosynthetic rates, and host–symbiont interactions may vary, with unforeseen impacts on the N isotopes. Moreover, fixed N may enter foraminifera through more than just feeding. Depending on the physiology of the endosymbionts, their host, and environmental conditions, direct nitrate uptake by the foraminifera host and/or its symbionts is a possibility (Piña-Ochoa et al., 2010; Uhle et al., 1999).

Regardless, the uniquely low FB-δ^{15}N of the dinoflagellate-bearing species supports higher photosynthetic rates (averaged over their lifetime) in dinoflagellate symbionts and, thus, a generally more important role for the symbiosis in the dinoflagellate-bearing species (e.g., as in *O. universa*; LeKieffre et al., 2020). The shallow depth (i.e., high-light) habitats of the dinoflagellate species are fully consistent with this interpretation, as is the dominance of dinoflagellate symbioses among modern symbiotic corals (Davy et al., 2012).

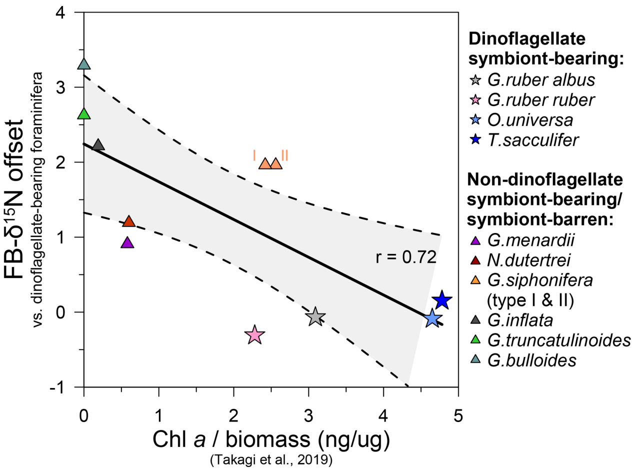

Figure 7. Chlorophyll *a* concentrations in living planktic foraminifera vs. FB-δ^{15}N offsets between dinoflagellate-bearing and other non-dinoflagellate-bearing foraminifera. Chlorophyll *a*/biomass values were measured in foraminifera collected in the central and western Pacific Ocean and the tropical eastern Atlantic Ocean across different seasons (Takagi et al., 2019) and compared to the median of the FB-δ^{15}N offsets in our core-top compilation (Figs. 5, S5; Table S2).

4.4 Deviations from the FB-δ^{15}N photosymbiosis paradigm at Site 516

Despite the overall consistency observed across sites in the global FB-δ^{15}N compilation, there are notable differences in interspecies offsets between the global compilation and DSDP Site 516 (Fig. 5a). In particular, among the foraminiferal species analyzed, the FB-δ^{15}N differences between the three dinoflagellate-bearing species and the three other species (*G. truncatulinoides*, *G. bulloides*, and *G. siphonifera*) are unusually great at DSDP Site 516 (Fig. 8). These differences warrant investigation here, with a focus on their cause and thus their implications for interspecies FB-δ^{15}N differences as a paleoproxy for foraminiferal photosymbiosis.

4.4.1 Depth habitat

The isotopic composition of suspended PN varies systematically with depth in the water column (Altabet, 1988; Altabet et al., 1991). Suspended PN has its lowest δ^{15}N in the euphotic layer, increasing with depth below the euphotic zone as a consequence of the preferential release of ^{14}N ammo-

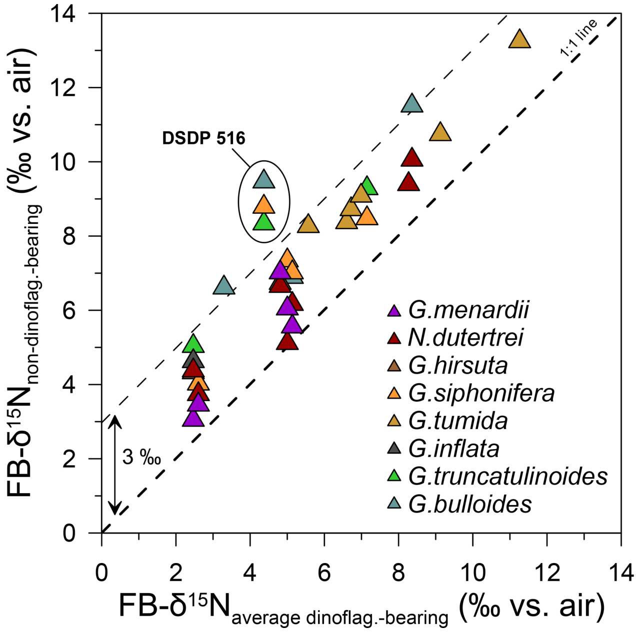

Figure 8. FB-δ^{15}N offsets between non-dinoflagellate-bearing foraminifera vs. dinoflagellate-bearing foraminifera (the average of *G. ruber albus*, *T. sacculifer*, and *O. universa*), with DSDP Site 516 having uniquely high FB-δ^{15}N offsets. DSDP Site 516 exhibits stronger ^{15}N enrichment for non-dinoflagellate-bearing foraminifera than other sites from the global core-top compilation (see Table S1 and Fig. S5).

nium during microbial decomposition. The PN δ^{15}N increase from the surface to ∼ 500 m depth can be up to 6 ‰ (Altabet, 1988; Altabet et al., 1991; Hannides et al., 2013). Therefore, planktic foraminifera living below the euphotic zone might be expected to have a higher δ^{15}N for their feeding source than surface dwellers.

At Site 516, our N isotope results show clear differences between two groups of species. The group of *G. truncatulinoides*, *G. bulloides*, and *G. siphonifera* have a δ^{15}N composition that is 3 ‰ to 5 ‰ higher than the group of *T. sacculifer* and *G. ruber*. These observations are in good agreement with previous studies (Ren et al., 2012b; Smart et al., 2018), including samples from upper-ocean net tows (surface 200 m), moored sediment traps, core tops, and down-core sediments. Planktic foraminifera living below the euphotic zone, when feeding on suspended PN, such as *G. truncatulinoides*, could incorporate food that is enriched in ^{15}N (Mintenbeck et al., 2007). To date, there are not yet any published depth profile data for PN or nitrate isotopes close to core Site 516. Based on data from the North Atlantic (Altabet, 1988; Altabet et al., 1991) and South Atlantic surface particles (Mino et al., 2002), PN δ^{15}N may be up to 9 ‰ higher at 1000 m water depth.

However, several lines of evidence suggest that depth habitat is not the main cause of the difference in δ^{15}N between the two groups. The two morpho- and genotypes of *G. siphonifera* (types I and II) are surface-to-thermocline dwellers (Bijma et al., 1990; Schiebel and Hemleben, 2017), but they have a higher δ^{15}N than the deeper-dwelling *G. truncatulinoides* (Hemleben et al., 1985) (Fig. 2a). Other differences in depth habitat inferred from foraminiferal δ^{18}O and δ^{13}C (Figs. S6 and S7 in the Supplement) are also not consistent with the interspecies δ^{15}N offsets that would be expected if depth were the main driver of FB-δ^{15}N. For example, of the species that we measured at Site 516, *G. truncatulinoides* is the deepest dweller according to its δ^{18}O values, but it has a δ^{15}N that is lower than that of *G. siphonifera* and *G. bulloides*. In addition, at DSDP Site 516, *G. siphonifera* δ^{15}N is more similar to *G. truncatulinoides* during interglacials but more similar to *G. bulloides* during glacials. However, the δ^{18}O of *G. siphonifera* maintains its position in δ^{18}O space relative to *T. sacculifer* and *G. ruber*, which would indicate no major change in the relative depth habitat of *G. siphonifera* through the glacial cycle. These observations suggest that depth habitat per se is not the main driver of the grouping that we see in the FB-δ^{15}N data. Depth also cannot explain the larger-than-average FB-δ^{15}N offset at Site 516, given the higher FB-δ^{15}N values for *G. siphonifera* and *G. bulloides* than for *G. truncatulinoides*.

4.4.2 Seasonality

Seasonality can also play a role in determining which nitrogen isotope signals are incorporated by foraminifera. While total foraminifera production often follows the seasonality of phytoplankton productivity in a given environment, there are major differences among species (Schiebel et al., 2001). In temperate latitudes and parts of the subtropical gyres, most nitrate supply from below occurs during the winter, with a nitrate-fueled phytoplankton bloom in the spring giving way to intensive ammonium recycling between phytoplankton and zooplankton in the summer–autumn (Dugdale and Goering, 1967; Eppley and Peterson, 1979). Depending on the most productive season of a given species of planktic foraminifera, it may feed within a nitrate-based or ammonium-based ecosystem, with the latter being associated with a lower δ^{15}N for suspended PN, zooplankton, and sinking PN (Fawcett et al., 2011). This distinction is apparent in the seasonality of foraminifera δ^{15}N (Smart et al., 2020, 2018). Thus, if we assume the seasonality of production is similar in the South Atlantic compared with the North Atlantic gyre, we would expect Site 516 summer bloomers *T. sacculifer* and *G. ruber* to be lower in δ^{15}N than *G. truncatulinoides*, which subsist in deep waters year-round but exhibit peak fluxes to the seafloor in winter–spring (Deuser, 1987; Hemleben et al., 1985; Salmon et al., 2015) when they reproduce in surface waters around the time of peak phytoplankton production (Schiebel et al., 2002; Reynolds et al., 2018). However, the offset that we observe between *T. sacculifer* and *G. ruber* vs. *G. truncatulinoides* is 4 ‰–4.5 ‰, which is substantially higher than typical seasonal offsets be-

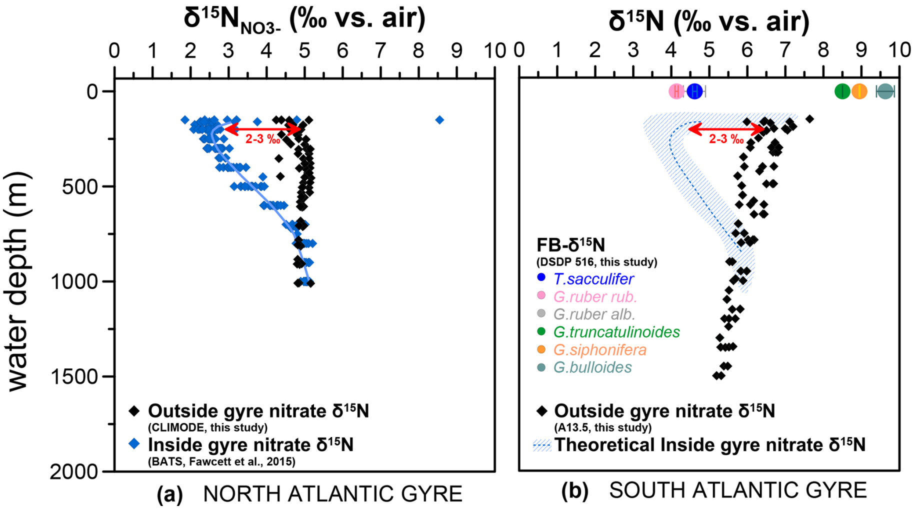

Figure 9. Estimation of the N isotopes of the South Atlantic gyre based on North Atlantic gyre nitrate isotopic measurements. **(a)** Seawater nitrate δ^{15}N in the North Atlantic gyre system, with distinct isotopic signatures outside (black diamonds, CLIMODE; this study) and inside (blue diamonds, BATS; Fawcett et al., 2015) the gyre system. **(b)** Seawater nitrate δ^{15}N from outside the South Atlantic gyre system (black diamonds, profile A13.5; this study). The hatched area with blue lines indicates the inferred possible seawater nitrate δ^{15}N for a location within the South Atlantic gyre, based on the difference between inside and outside the North Atlantic gyre and the nitrate isotopic data from the South Atlantic. Colored circles indicate Holocene FB-δ^{15}N from Site 516. Locations for seawater nitrate δ^{15}N profiles are shown in Fig. 1.

tween summer and winter PN δ^{15}N in oligotrophic regions (e.g., Smart et al., 2018). Thus, if seasonality is the explanation for the particularly large FB-δ^{15}N interspecies offsets at DSDP Site 516, it would appear that some special source of seasonality is required for the South Atlantic subtropical gyre.

4.4.3 Lateral transport

In austral winter–spring, between July and September, the oligotrophic South Atlantic gyre is affected by wind-driven mixing and an Ekman-transport-driven incursion of nutrient-rich waters with high-δ^{15}N nitrate from the Southern Ocean (Figs. 1, S8). *Globigerina bulloides*, perhaps the most opportunistic among the species discussed here, is abundant at the southern margin of the Atlantic subtropical gyre around 35° S (Boltovskoy, 1962), thus recording the higher δ^{15}N associated with high degrees of consumption of a nitrate source with a δ^{15}N that is similar to that of Subantarctic Mode Water (Smart et al., 2015). Indeed, it has been shown that *G. bulloides* reaches highest abundances when food supply is increased (Kretschmer et al., 2018; Mortyn and Charles, 2003; Schiebel et al., 1995). *Globigerinella siphonifera*, although it is a subtropical species, similarly yields the highest shell fluxes at times of highest productivity (Jonkers and Kučera, 2015), which would be the winter–spring season in the South Atlantic. For both *G. bulloides* and *G. siphonifera*, we observed highly variable specimen counts across the last 160 kyr (Fig. S9), in strong contrast to the uniformly high abundances of *T. sacculifer*, *G. ruber albus*, and *G. truncatulinoides* throughout the record. Therefore, the large FB-δ^{15}N offset between summer-blooming species (*T. sacculifer* and *G. ruber*) and *G. bulloides* and *G. siphonifera* at Site 516 could reflect increased nutrient influx from the Southern Ocean with an elevated δ^{15}N signature in austral winter–spring during northward movement of the subtropical front. As previously documented, not only nutrients but also planktic foraminifera and/or their particulate food sources (PN) can be transported from other oceanic regions to the South Atlantic (Peeters et al., 2004; Smart et al., 2020; Granger et al., 2024).

Here, we compare the nitrate profiles for "inside-gyre" (BATS; Fawcett et al., 2015) vs. "outside-gyre" (CLIMODE; this study) stations in the North Atlantic (Fig. 9a) to evaluate baseline (nitrate δ^{15}N) differences between the two regions, providing a reference point for the baseline (nitrate δ^{15}N) differences that we could expect in the South Atlantic. Subsurface nitrate at 200 m inside the North Atlantic gyre is ca. 3 ‰ lower than subsurface nitrate outside the gyre, which is due to gyre-related N_2-fixation processes keeping thermocline nitrate δ^{15}N low. A similar upper-ocean nitrate δ^{15}N gradient is observed in other subtropical gyres in the Indian and Pacific oceans, with ~ 2.5 ‰ lower δ^{15}N inside the gyre vs. outside (Harms et al., 2019; Yoshikawa et al., 2018, 2015; Marconi et al., 2024; Marshall et al., 2023). While no similar data exist from inside the South Atlantic gyre, a hypothetical inside-gyre δ^{15}N profile based on the southern outside gyre would put the subsurface nitrate δ^{15}N at 4 ‰ (inside gyre) vs. 7 ‰ (outside gyre) (Fig. 9b), closely matching the FB-δ^{15}N of *T. sacculifer* and *G. ruber* at Site 516. Symbiont-

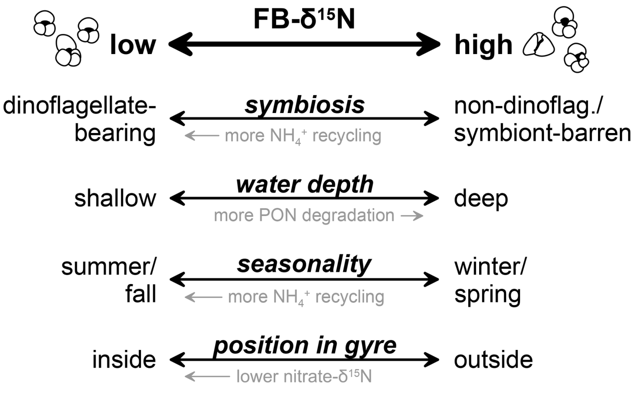

Figure 10. Proposed different processes affecting FB-δ^{15}N at DSDP Site 516. Shallow-dwelling, summer-blooming, dinoflagellate-bearing foraminifera located within the oligotrophic gyre record generally lower FB-δ^{15}N values than symbiont-barren foraminifera or foraminifera hosting symbionts other than dinoflagellates that generally live in a deeper (depth) habitat, bloom during the winter/spring season, and/or live outside oligotrophic gyres. PON stands for particulate organic nitrogen.

barren *G. truncatulinoides* has the expected ~ 3 ‰ δ^{15}N offset above inside-gyre nitrate, i.e., the full trophic enrichment typically observed for marine zooplankton (Minagawa and Wada, 1984). *G. bulloides* and *G. siphonifera*, in contrast, appear to be elevated by an additional 1 ‰–2 ‰. This additional offset could be due to a Southern Ocean (i.e., outside-gyre) influence, where subsurface nitrate derived from Subantarctic Mode Water is enriched in ^{15}N due to incomplete nutrient consumption (Sigman et al., 2000; Smart et al., 2015). Indeed, the distinct δ^{13}C of *G. bulloides* has been interpreted as reflecting its Southern Ocean origin (Fig. S7 in the Supplement; Ninnemann and Charles, 1997). In our interpretation, both the relatively high δ^{15}N of subantarctic-sourced nitrate and the greater potential for the incursion of extra-subtropical water into the small South Atlantic gyre contribute to the abnormally large FB-δ^{15}N difference at DSDP Site 516 between *G. bulloides/G. siphonifera* and the dinoflagellate-bearing species. The South Atlantic may be more prone to these effects than the North Atlantic gyre or other sites from the core-top compilation due to the smaller geographic extent of the gyre and/or its proximity to the Southern Ocean.

5 Conclusions

FB-δ^{15}N is a promising new geochemical tool to identify fossil foraminiferal photosymbiosis, particularly the strong symbiosis with dinoflagellates, and also has the potential to identify symbiosis with non-dinoflagellate symbionts (e.g., chrysophytes and pelagophytes) (Figs. 5, 6, 10). The FB-δ^{15}N range of the non-dinoflagellate symbiont group may indicate that non-dinoflagellate symbioses in foraminifera are relatively weak in terms of the internal N demand that they generate, which could indicate that they generate substantially less photosynthetic energy for the host compared with dinoflagellate endosymbionts. This possibility warrants testing with other approaches.

While FB-δ^{15}N offsets are remarkably consistent in our global compilation, DSDP Site 516 stands out for its larger-than-expected FB-δ^{15}N offsets between the dinoflagellate-bearing foraminifera (*G. ruber* and *T. sacculifer*) and the non-dinoflagellate-bearing *G. siphonifera* and *G. bulloides*. Site 516 sits near the core of the uniquely small South Atlantic subtropical gyre. As a subtropical gyre, it hosts convergence, fed by inflow from the surrounding surface ocean. Accordingly, we propose that DSDP Site 516 is influenced by the input to the region of *G. bulloides* and *G. siphonifera* specimens and/or their N sources that were sourced from the higher-δ^{15}N nitrate of the subantarctic zone to the south and/or the more proximal temperate ocean waters surrounding the gyre. With this caveat regarding regions with strong environmental gradients, our findings support the use of interspecies FB-δ^{15}N offsets to investigate the emergence and evolution of photosymbiosis in foraminifera and potentially other animals.

Data availability. The data are available in the Supplement and on PANGAEA (https://doi.org/10.1594/PANGAEA.979691, Auderset et al., 2025).

Supplement. The supplement related to this article is available online at https://doi.org/10.5194/bg-22-1887-2025-supplement.

Author contributions. AA and AMG designed the study. AA measured foraminifera-bound nitrogen isotopes in the lab of AMG. YR and DM measured seawater nitrate nitrogen isotopes. AA, SMS, DMS, and AMG wrote the manuscript. All authors contributed to the interpretation of the data and provided input on the final manuscript at different stages of the project.

Competing interests. The contact author has declared that none of the authors has any competing interests.

Acknowledgements. The authors wish to thank Björn Taphorn for micropaleontological assistance and Florian Rubach, Barbara Hinnenberg, and Mareike Schmitt for technical support. We are also grateful to Rocco Gennari and the anonymous reviewer for their insightful comments.

Financial support. This work was funded by the Max Planck Society and SNSF mobility grant P2EZP2_200000. Yeongjun Ryu, Dario Marconi, and Daniel M. Sigman were funded by US NSF OCE (grant nos. 0960802, 10011610, 10014342, 10014700, 10015689, 1060947, and 1136345).

The article processing charges for this open-access publication were covered by the Max Planck Society.

Review statement. This paper was edited by Carolin Löscher and reviewed by Rocco Gennari and one anonymous referee.

References

Altabet, M.: Variations in nitrogen isotopic composition between sinking and suspended particles: implications for nitrogen cycling and particle transformation in the open ocean, Deep-Sea Res. Pt. I, 35, 535–554, https://doi.org/10.1016/0198-0149(88)90130-6, 1988.

Altabet, M. and Francois, R.: The use of nitrogen isotopic ratio for reconstruction of past changes in surface ocean nutrient utilization, in: Carbon Cycling in the Glacial Ocean: Constraints on the Ocean's Role in Global Change: Quantitative Approaches in Paleoceanography, Springer, 281–306, https://doi.org/10.1007/978-3-642-78737-9_12, 1994.

Altabet, M. A., Deuser, W. G., Honjo, S., and Stienen, C.: Seasonal and depth-related changes in the source of sinking particles in the North Atlantic, Nature, 354, 136, https://doi.org/10.1038/354136a0, 1991.

Anderson, O., Spindler, M., Bé, A., and Hemleben, C.: Trophic activity of planktonic foraminifera, J. Mar. Biol. Assoc. UK, 59, 791–799, https://doi.org/10.1017/S002531540004577X, 1979.

Anderson, O. R. and Be, A. W.: The ultrastructure of a planktonic foraminifer, Globigerinoides sacculifer (Brady), and its symbiotic dinoflagellates, J. Foramin. Res., 6, 1–21, https://doi.org/10.2113/gsjfr.6.1.1, 1976.

Auderset, A., Moretti, S., Taphorn, B., Ebner, P.-R., Kast, E., Wang, X. T., Schiebel, R., Sigman, D. M., Haug, G. H., and Martínez-García, A.: Enhanced ocean oxygenation during Cenozoic warm periods, Nature, 609, 77–82, https://doi.org/10.1038/s41586-022-05017-0, 2022.

Auderset, A., Fripiat, F. o., Creel, R. C., Oesch, L., Studer, A. S., Repschläger, J., Hathorne, E., Vonhof, H., Schiebel, R., and Gordon, L.: Sea Level Modulation of Atlantic Nitrogen Fixation Over Glacial Cycles, Paleoceanogr. Paleocl., 39, e2024PA004878, https://doi.org/10.1029/2024PA004878, 2024.

Auderset, A., Smart, S. M., Ryu, Y., Marconi, D., Ren, H. A., Heins, L., Vonhof, H., Schiebel, R., Repschläger, J., Vonhof, H. B., Schiebel, R., Sigman, D. M., Haug, G. H., and Martínez-García, A.: Species-specific foraminifera-bound nitrogen isotope and foraminiferal calcite oxygen and carbon isotope measurements from DSDP Site 516 in the South Atlantic over a glacial-interglacial cycle, PANGAEA [data set], https://doi.org/10.1594/PANGAEA.979691, 2025.

Bijma, J., Faber, W. W., and Hemleben, C.: Temperature and salinity limits for growth and survival of some planktonic foraminifers in laboratory cultures, J. Foramin. Res., 20, 95–116, https://doi.org/10.2113/gsjfr.20.2.95, 1990.

Bijma, J., Hemleben, C., Huber, B. T., Erlenkeuser, H., and Kroon, D.: Experimental determination of the ontogenetic stable isotope variability in two morphotypes of Globigerinella siphonifera (d'Orbigny), Marine Micropaleontol., 35, 141–160, https://doi.org/10.1016/S0377-8398(98)00017-6, 1998.

Bird, C., Darling, K. F., Russell, A. D., Davis, C. V., Fehrenbacher, J., Free, A., Wyman, M., and Ngwenya, B. T.: Cyanobacterial endobionts within a major marine planktonic calcifier (Globigerina bulloides, Foraminifera) revealed by 16S rRNA metabarcoding, Biogeosciences, 14, 901–920, https://doi.org/10.5194/bg-14-901-2017, 2017.

Bird, C., LeKieffre, C., Jauffrais, T., Meibom, A., Geslin, E., Filipsson, H. L., Maire, O., Russell, A. D., and Fehrenbacher, J. S.: Heterotrophic Foraminifera Capable of Inorganic Nitrogen Assimilation, Front. Microbiol., 11, 3076, https://doi.org/10.3389/fmicb.2020.604979, 2020.

Boltovskoy, E.: Planktonic foraminifera as indicators of different water masses in the South Atlantic, Micropaleontology, 8, 403–408, https://doi.org/10.2307/1484531, 1962.

Brandes, J. A. and Devol, A. H.: A global marine-fixed nitrogen isotopic budget: Implications for Holocene nitrogen cycling, Global Biogeochem. Cycles, 16, 67-61–67-14, https://doi.org/10.1029/2001GB001856, 2002.

Breitenbach, S. F. and Bernasconi, S. M.: Carbon and oxygen isotope analysis of small carbonate samples (20 to 100 µg) with a GasBench II preparation device, Rapid Commun. Mass Sp., 25, 1910–1914, https://doi.org/10.1002/rcm.5052, 2011.

Broecker, W. S.: Glacial to interglacial changes in ocean chemistry, Prog. Oceanogr., 11, 151–197, https://doi.org/10.1016/0079-6611(82)90007-6, 1982.

Broecker, W. S. and Henderson, G. M.: The sequence of events surrounding Termination II and their implications for the cause of glacial-interglacial CO_2 changes, Paleoceanography, 13, 352–364, https://doi.org/10.1029/98PA00920, 1998.

Brunelle, B. G., Sigman, D. M., Cook, M. S., Keigwin, L. D., Haug, G. H., Plessen, B., Schettler, G., and Jaccard, S. L.: Evidence from diatom-bound nitrogen isotopes for subarctic Pacific stratification during the last ice age and a link to North Pacific denitrification changes, Paleoceanography, 22, PA1215, https://doi.org/10.1029/2005PA001205, 2007.

Casciotti, K. L., Trull, T. W., Glover, D. M., and Davies, D.: Constraints on nitrogen cycling at the subtropical North Pacific Station ALOHA from isotopic measurements of nitrate and particulate nitrogen, Deep-Sea Res. Pt. II: Topical Studies in Oceanography, 55, 1661–1672, https://doi.org/10.1016/j.dsr2.2008.04.017, 2008.

Casciotti, K. L., Sigman, D. M., Hastings, M. G., Böhlke, J., and Hilkert, A.: Measurement of the oxygen isotopic composition of nitrate in seawater and freshwater using the denitrifier method, Anal. Chem., 74, 4905–4912, https://doi.org/10.1021/ac020113w, 2002.

Cole, J. and Villacastin, C.: Sea surface temperature variability in the northern Benguela upwelling system, and implications for fisheries research, Int. J. Remote Sens., 21, 1597–1617, https://doi.org/10.1080/014311600209922, 2000.

Costa, K. M., McManus, J. F., Anderson, R. F., Ren, H., Sigman, D. M., Winckler, G., Fleisher, M. Q., Marcantonio, F., and Ravelo, A. C.: No iron fertilization in the equatorial Pacific Ocean during the last ice age, Nature, 529, 519–522, https://doi.org/10.1038/nature16453, 2016.

Cullen, J. J., Franks, P. J., Karl, D. M., and Longhurst, A.: Physical influences on marine ecosystem dynamics, The Sea, 12, 297–336, 2002.

Davy, S. K., Allemand, D., and Weis Virginia, M.: Cell Biology of Cnidarian-Dinoflagellate Symbiosis, Microbiol. Mol. Biol. R., 76, 229–261, https://doi.org/10.1128/mmbr.05014-11, 2012.

DeNiro, M. J.: You are what you eat (plus a few ‰): the carbon isotope cycle in food chains, Geological Society of America Abstracts with Programs, Geological Society of America Abstracts with Programs, 8, 834–835, 1976.

DeNiro, M. J. and Epstein, S.: Influence of diet on the distribution of nitrogen isotopes in animals, Geochim. Cosmochim. Ac., 45, 341–351, https://doi.org/10.1016/0016-7037(81)90244-1, 1981.

Deuser, W.: Seasonal variations in isotopic composition and deep-water fluxes of the tests of perennially abundant planktonic foraminifera of the Sargasso Sea; results from sediment-trap collections and their paleoceanographic significance, J. Foramin. Res., 17, 14–27, 1987.

Deutsch, C., Sigman, D. M., Thunell, R. C., Meckler, A. N., and Haug, G. H.: Isotopic constraints on glacial/interglacial changes in the oceanic nitrogen budget, Global Biogeochem. Cycles, 18, GB4012, https://doi.org/10.1029/2003GB002189, 2004.

D'Hondt, S., Zachos, J. C., and Schultz, G.: Stable isotopic signals and photosymbiosis in late Paleocene planktic foraminifera, Paleobiology, 20, 391–406, https://doi.org/10.1017/S0094837300012847, 1994.

Dugdale, R. C. and Goering, J. J.: Uptake of new and regenerated forms of nitrogen in primary productivity, Limnol. Oceanogr., 12, 196–206, https://doi.org/10.4319/lo.1967.12.2.0196, 1967.

Edgar, K. M., Bohaty, S., Gibbs, S., Sexton, P., Norris, R., and Wilson, P.: Symbiont 'bleaching'in planktic foraminifera during the Middle Eocene Climatic Optimum, Geology, 41, 15–18, https://doi.org/10.1130/G33388.1, 2013.

Eppley, R. W. and Peterson, B. J.: Particulate organic matter flux and planktonic new production in the deep ocean, Nature, 282, 677–680, https://doi.org/10.1038/282677a0, 1979.

Ezard, T. H., Edgar, K. M., and Hull, P. M.: Environmental and biological controls on size-specific δ13C and δ18O in recent planktonic foraminifera, Paleoceanography, 30, 151–173, https://doi.org/10.1002/2014PA002735, 2015.

Faber, W., Anderson, O., Lindsey, J., and Caron, D.: Algal-foraminiferal symbiosis in the planktonic foraminifer Globigerinella aequilateralia; I, Occurrence and stability of two mutually exclusive chrysophyte endosymbionts and their ultrastructure, J. Foramin. Res., 18, 334–343, https://doi.org/10.2113/gsjfr.18.4.334, 1988.

Faber, W., Anderson, O., and Caron, D.: Algal-foraminiferal symbiosis in the planktonic foraminifer Globigerinella aequilateralis; II, Effects of two symbiont species on foraminiferal growth and longevity, J. Foramin. Res., 19, 185–193, https://doi.org/10.2113/gsjfr.19.3.185, 1989.

Fairbanks, R. G. and Wiebe, P. H.: Foraminifera and chlorophyll maximum: vertical distribution, seasonal succession, and paleoceanographic significance, Science, 209, 1524–1526, 1980.

Falkowski, P. G.: Evolution of the nitrogen cycle and its influence on the biological sequestration of CO_2 in the ocean, Nature, 387, 272, https://doi.org/10.1038/387272a0, 1997.

Fawcett, S. E., Lomas, M. W., Casey, J. R., Ward, B. B., and Sigman, D. M.: Assimilation of upwelled nitrate by small eukaryotes in the Sargasso Sea, Nat. Geosci., 4, 717–722, https://doi.org/10.1038/ngeo1265, 2011.

Fawcett, S. E., Ward, B. B., Lomas, M. W., and Sigman, D. M.: Vertical decoupling of nitrate assimilation and nitrification in the Sargasso Sea, Deep-Sea Res. Pt. I, 103, 64–72, https://doi.org/10.1016/j.dsr.2015.05.004, 2015.

Febvre-Chevalier, C.: Constitution ultrastructurale de Globigerina bulloides d'Orbigny, 1826 (Rhizopoda-Foraminifera), Protistologica, 7, 311–324, 1971.

Fripiat, F., Martínez-García, A., Marconi, D., Fawcett, S. E., Kopf, S. H., Luu, V. H., Rafter, P. A., Zhang, R., Sigman, D. M., and Haug, G. H.: Nitrogen isotopic constraints on nutrient transport to the upper ocean, Nat. Geosci., 14, 855–861, https://doi.org/10.1038/s41561-021-00836-8, 2021.

Galbraith, E. D., Kienast, M., Albuquerque, A. L., Altabet, M. A., Batista, F., Bianchi, D., Calvert, S. E., Contreras, S., Crosta, X., and De Pol-Holz, R.: The acceleration of oceanic denitrification during deglacial warming, Nat. Geosci., 6, 579, https://doi.org/10.1038/ngeo1832, 2013.

Garcia, H. E., Locarnini, R. A., Boyer, T. P., Antonov, J. I., Baranova, O. K., Zweng, M. M., Reagan, J. R., and Johnson, D. R.: World Ocean Atlas 2013, Volume 4: Dissolved Inorganic Nutrients (phosphate, nitrate, silicate), S. Levitus, edited by: Mishonov, A., NOAA Atlas NESDIS, 76, 25 pp., 2014.

Gast, R. and Caron, D.: Molecular phylogeny of symbiotic dinoflagellates from planktonic foraminifera and radiolaria, Mol. Biol. Evol., 13, 1192–1197, https://doi.org/10.1093/oxfordjournals.molbev.a025684, 1996.

Gast, R. J., McDonnell, T. A., and Caron, D. A.: srDna-based taxonomic affinities of algal symbionts from a planktonic foraminifer and a solitary radiolarian, J. Phycol., 36, 172–177, https://doi.org/10.1046/j.1529-8817.2000.99133.x, 2000.

Gastrich, M. D.: Ultrastructure of a new intracellular symbiotic alga found within planktonic foraminifera, J. Phycol., 23, 623–632, https://doi.org/10.1111/j.1529-8817.1987.tb04215.x, 1987.

Granger, J. and Sigman, D. M.: Removal of nitrite with sulfamic acid for nitrate N and O isotope analysis with the denitrifier method, Rapid Commun. Mass Sp., 23, 3753–3762, https://doi.org/10.1002/rcm.4307, 2009.

Granger, R., Smart, S. M., Foreman, A., Auderset, A., Campbell, E. C., Marshall, T. A., Haug, G. H., Sigman, D. M., Martínez-García, A., and Fawcett, S. E.: Tracking Agulhas Leakage in the South Atlantic Using Modern Planktic Foraminifera Nitrogen Isotopes, Geochem. Geophys. Geosyst., 25, e2023GC011190, https://doi.org/10.1029/2023GC011190, 2024.

Gruber, N. and Sarmiento, J. L.: Global patterns of marine nitrogen fixation and denitrification, Global Biogeochem. Cycles, 11, 235–266, https://doi.org/10.1029/97GB00077, 1997.

Hallock, P.: Algal symbiosis: a mathematical analysis, Marine Biol., 62, 249–255, https://doi.org/10.1007/BF00397691, 1981.

Hannides, C. C. S., Popp, B. N., Choy, C. A., and Drazen, J. C.: Midwater zooplankton and suspended particle dynamics in the North Pacific Subtropical Gyre: A stable isotope perspective, Limnol. Oceanogr., 58, 1931–1946, https://doi.org/10.4319/lo.2013.58.6.1931, 2013.

Harms, N. C., Lahajnar, N., Gaye, B., Rixen, T., Dähnke, K., Ankele, M., Schwarz-Schampera, U., and Emeis, K.-C.: Nutrient distribution and nitrogen and oxygen isotopic composition of nitrate in water masses of the subtropical southern Indian Ocean, Biogeosciences, 16, 2715–2732, https://doi.org/10.5194/bg-16-2715-2019, 2019.

Hemleben, C., Spindler, M., Breitinger, I., and Deuser, W. G.: Field and laboratory studies on the ontogeny and ecology of some globorotaliid species from the Sargasso Sea off Bermuda, J. Foramin. Res., 15, 254–272, https://doi.org/10.2113/gsjfr.15.4.254, 1985.

Hemleben, C., Spindler, M., and Anderson, O. R.: Modern planktonic foraminifera, Springer Science & Business Media, https://doi.org/10.1007/978-1-4612-3544-6, 1989.

Hess, A. V., Auderset, A., Rosenthal, Y., Miller, K. G., Zhou, X., Sigman, D. M., and Martínez-García, A.: A well-oxygenated eastern tropical Pacific during the warm Miocene, Nature, 619, 521–525, https://doi.org/10.1038/s41586-023-06104-6, 2023.

Hohmann-Marriott, M. F. and Blankenship, R. E.: Evolution of photosynthesis, Annu. Rev. Plant Biol., 62, 515–548, https://doi.org/10.1146/annurev-arplant-042110-103811, 2011.

Hupp, B. N., Kelly, D. C., Zachos, J. C., and Bralower, T. J.: Effects of size-dependent sediment mixing on deep-sea records of the Paleocene-Eocene Thermal Maximum, Geology, 47, 749–752, https://doi.org/10.1130/G46042.1, 2019.

Hutto, L., Weller, R., Fratantoni, D., Lord, J., Kemp, J., Lund, J., Brambilla, E., and Bigorre, S.: CLIVAR Mode Water Dynamics Experiment (CLIMODE) fall 2005, R/V Oceanus voyage 419, November 9, 2005 – November 27, 2005, Woods Hole Oceanographic Institution, https://doi.org/10.1575/1912/1073, 2006.

Jonkers, L. and Kučera, M.: Global analysis of seasonality in the shell flux of extant planktonic Foraminifera, Biogeosciences, 12, 2207–2226, https://doi.org/10.5194/bg-12-2207-2015, 2015.

Kast, E. R., Stolper, D. A., Auderset, A., Higgins, J. A., Ren, H., Wang, X. T., Martínez-García, A., Haug, G. H., and Sigman, D. M.: Nitrogen isotope evidence for expanded ocean suboxia in the early Cenozoic, Science, 364, 386–389, https://doi.org/10.1126/science.aau5784, 2019.

Kast, E. R., Griffiths, M. L., Kim, S. L., Rao, Z. C., Shimada, K., Becker, M. A., Maisch, H. M., Eagle, R. A., Clarke, C. A., and Neumann, A. N.: Cenozoic megatooth sharks occupied extremely high trophic positions, Sci. Adv., 8, eabl6529, https://doi.org/10.1126/sciadv.abl6529, 2022.

Knapp, A. N., Sigman, D. M., and Lipschultz, F.: N isotopic composition of dissolved organic nitrogen and nitrate at the Bermuda Atlantic Time-series Study site, Global Biogeochem. Cycles, 19, GB1018, https://doi.org/10.1029/2004GB002320, 2005.

Knapp, A. N., DiFiore, P. J., Deutsch, C., Sigman, D. M., and Lipschultz, F.: Nitrate isotopic composition between Bermuda and Puerto Rico: Implications for N_2 fixation in the Atlantic Ocean, Global Biogeochem. Cycles, 22, GB3014, https://doi.org/10.1029/2007GB003107, 2008.

Kretschmer, K., Jonkers, L., Kucera, M., and Schulz, M.: Modeling seasonal and vertical habitats of planktonic foraminifera on a global scale, Biogeosciences, 15, 4405–4429, https://doi.org/10.5194/bg-15-4405-2018, 2018.

Kroopnick, P.: The distribution of 13C of ΣCO_2 in the world oceans, Deep-Sea Res. Pt. I, 32, 57–84, https://doi.org/10.1016/0198-0149(85)90017-2, 1985.

Lee, J. J., Freudenthal, H. D., Kossoy, V., and Bé, A.: Cytological observations on two planktonic foraminifera, Globigerina bulloides d'Orbigny, 1826, and Globigerinoides ruber (d'Orbigny, 1839) Cushman, 1927, J. Protozool., 12, 531–542, https://doi.org/10.1111/j.1550-7408.1965.tb03253.x, 1965.

LeKieffre, C., Spero, H. J., Fehrenbacher, J. S., Russell, A. D., Ren, H., Geslin, E., and Meibom, A.: Ammonium is the preferred source of nitrogen for planktonic foraminifer and their dinoflagellate symbionts, P. Roy. Soc. B, 287, 20200620, https://doi.org/10.1098/rspb.2020.0620, 2020.

Li, D.-W., Xiang, R., Wu, Q., and Kao, S.-J.: Planktic foraminifera-bound organic nitrogen isotopic composition in contemporary water column and sediment trap, Deep-Sea Res. Pt. I, 143, 28–34, https://doi.org/10.1016/j.dsr.2018.12.003, 2019.

Lisiecki, L. E. and Raymo, M. E.: A Pliocene-Pleistocene stack of 57 globally distributed benthic δ18O records, Paleoceanography, 20, PA1003, https://doi.org/10.1029/2004PA001071, 2005.

Lisiecki, L. E. and Stern, J. V.: Regional and global benthic δ18O stacks for the last glacial cycle, Paleoceanography, 31, 1368–1394, https://doi.org/10.1002/2016PA003002, 2016.

Liu, K.-K., Su, M.-J., Hsueh, C.-R., and Gong, G.-C.: The nitrogen isotopic composition of nitrate in the Kuroshio Water northeast of Taiwan: Evidence for nitrogen fixation as a source of isotopically light nitrate, Marine Chem., 54, 273–292, https://doi.org/10.1016/0304-4203(96)00034-5, 1996.

Lomas, M., Bates, N., Johnson, R., Knap, A., Steinberg, D., and Carlson, C.: Two decades and counting: 24-years of sustained open ocean biogeochemical measurements in the Sargasso Sea, Deep-Sea Res. Pt. II, 93, 16–32, https://doi.org/10.1016/j.dsr2.2013.01.008, 2013.

Lueders-Dumont, J. A., Wang, X. T., Jensen, O. P., Sigman, D. M., and Ward, B. B.: Nitrogen isotopic analysis of carbonate-bound organic matter in modern and fossil fish otoliths, Geochim. Cosmochim. Ac., 224, 200–222, https://doi.org/10.1016/j.gca.2018.01.001, 2018.

Marconi, D., Weigand, M. A., Rafter, P. A., McIlvin, M. R., Forbes, M., Casciotti, K. L., and Sigman, D. M.: Nitrate isotope distributions on the US GEOTRACES North Atlantic cross-basin section: Signals of polar nitrate sources and low latitude nitrogen cycling, Marine Chem., 177, 143–156, https://doi.org/10.1016/j.marchem.2015.06.007, 2015.

Marconi, D., Sigman, D. M., Casciotti, K. L., Campbell, E. C., Alexandra Weigand, M., Fawcett, S. E., Knapp, A. N., Rafter, P. A., Ward, B. B., and Haug, G. H.: Tropical dominance of N_2 fixation in the North Atlantic Ocean, Global Biogeochem. Cycles, 31, 1608–1623, https://doi.org/10.1002/2016GB005613, 2017.

Marconi, D., Sigman, D. M., Casciotti, K. L., Lawrence, R. M., Wang, W., Oleynik, S., and Martínez-García, A.: Distinguishing the isotopic signals of nitrate assimilation and denitrification along meridional Pacific section US GEOTRACES GP15, ESS Open Archive, 12 November 2024..

Marshall, T., Granger, J., Casciotti, K. L., Dähnke, K., Emeis, K.-C., Marconi, D., McIlvin, M. R., Noble, A. E., Saito, M. A., and Sigman, D. M.: The Angola Gyre is a hotspot of dinitrogen fixation in the South Atlantic Ocean, Commun. Earth Environ., 3, 151, https://doi.org/10.1038/s43247-022-00474-x, 2022.

Marshall, T. A., Sigman, D. M., Beal, L. M., Foreman, A., Martínez-García, A., Blain, S., Campbell, E., Fripiat, F., Granger, R., and Harris, E.: The Agulhas Current transports signals of local and remote Indian Ocean nitrogen cycling, J. Geophys. Res.-Oceans, 128, e2022JC019413, https://doi.org/10.1029/2022JC019413, 2023.

Martínez-García, A., Sigman, D. M., Ren, H., Anderson, R. F., Straub, M., Hodell, D. A., Jaccard, S. L., Eglinton, T. I., and Haug, G. H.: Iron fertilization of the Subantarctic Ocean during the last ice age, Science, 343, 1347–1350, https://doi.org/10.1126/science.1246848, 2014.

Martínez-García, A., Jung, J., Ai, X. E., Sigman, D. M., Auderset, A., Duprey, N. N., Foreman, A., Fripiat, F., Leichliter, J., and Lüdecke, T.: Laboratory assessment of the impact of chemical oxidation, mineral dissolution, and heating on the nitrogen isotopic composition of fossil-bound organic matter, Geochem. Geophys. Geosyst., 23, e2022GC010396, https://doi.org/10.1029/2022GC010396, 2022.

McElroy, M. B.: Marine biological controls on atmospheric CO_2 and climate, Nature, 302, 328–329, https://doi.org/10.1038/302328a0, 1983.

Meckler, A. N., Ren, H., Sigman, D. M., Gruber, N., Plessen, B., Schubert, C. J., and Haug, G. H.: Deglacial nitrogen isotope changes in the Gulf of Mexico: Evidence from bulk sedimentary and foraminifera-bound nitrogen in Orca Basin sediments, Paleoceanography, 26, PA4216, https://doi.org/10.1029/2011PA002156, 2011.

Minagawa, M. and Wada, E.: Stepwise enrichment of 15N along food chains: further evidence and the relation between δ15N and animal age, Geochim. Cosmochim. Ac., 48, 1135–1140, https://doi.org/10.1016/0016-7037(84)90204-7, 1984.

Mino, Y., Saino, T., Suzuki, K., and Marañón, E.: Isotopic composition of suspended particulate nitrogen (δ15Nsus) in surface waters of the Atlantic Ocean from 50° N to 50° S, Global Biogeochem. Cycles, 16, 7-1–7-9, https://doi.org/10.1029/2001GB001635, 2002.

Mintenbeck, K., Jacob, U., Knust, R., Arntz, W., and Brey, T.: Depth-dependence in stable isotope ratio δ15N of benthic POM consumers: the role of particle dynamics and organism trophic guild, Deep-Sea Res. Pt. I, 54, 1015–1023, https://doi.org/10.1016/j.dsr.2007.03.005, 2007.

Möbius, J.: Isotope fractionation during nitrogen remineralization (ammonification): Implications for nitrogen isotope biogeochemistry, Geochim. Cosmochim. Ac., 105, 422–432, https://doi.org/10.1016/j.gca.2012.11.048, 2013.

Montoya, J. P., Carpenter, E. J., and Capone, D. G.: Nitrogen fixation and nitrogen isotope abundances in zooplankton of the oligotrophic North Atlantic, Limnol. Oceanogr., 47, 1617–1628, https://doi.org/10.4319/lo.2002.47.6.1617, 2002.

Moretti, S., Duprey, N. N., Foreman, A. D., Arns, A., Brömme, S., Jung, J., Ai, X. E., Auderset, A., Bieler, A. L., and Eck, C.: Analytical improvements and assessment of long-term performance of the oxidation–denitrifier method, Rapid Commun. Mass Sp., 38, e9650, https://doi.org/10.1002/rcm.9650, 2024.

Mortyn, P. G. and Charles, C. D.: Planktonic foraminiferal depth habitat and δ18O calibrations: Plankton tow results from the Atlantic sector of the Southern Ocean, Paleoceanography, 18, 1037, https://doi.org/10.1029/2001PA000637, 2003.

Mulitza, S., Dürkoop, A., Hale, W., Wefer, G., and Stefan Niebler, H.: Planktonic foraminifera as recorders of past surface-water stratification, Geology, 25, 335–338, https://doi.org/10.1130/0091-7613(1997)025<0335:PFAROP>2.3.CO;2, 1997.

Ninnemann, U. S. and Charles, C. D.: Regional differences in Quaternary Subantarctic nutrient cycling: Link to intermediate and deep water ventilation, Paleoceanography, 12, 560–567, https://doi.org/10.1029/97PA01032, 1997.

Norris, R. D.: Symbiosis as an evolutionary innovation in the radiation of Paleocene planktic foraminifera, Paleobiology, 22, 461–480, https://doi.org/10.1017/S0094837300016468, 1996.

Norris, R. D.: Recognition and macroevolutionary significance of photosymbiosis in molluscs, corals, and foraminifera, The Paleontological Society Papers, 4, 68–100, https://doi.org/10.1017/S1089332600000401, 1998.

Paillard, D., Labeyrie, L., and Yiou, P.: Macintosh program performs time-series analysis, Eos, Transactions American Geophysical Union, 77, 379–379, 1996.

Peeters, F. J., Acheson, R., Brummer, G.-J. A., De Ruijter, W. P., Schneider, R. R., Ganssen, G. M., Ufkes, E., and Kroon, D.: Vigorous exchange between the Indian and Atlantic oceans at the end of the past five glacial periods, Nature, 430, 661–665, https://doi.org/10.1038/nature02785, 2004.

Peterson, R. G. and Stramma, L.: Upper-level circulation in the South Atlantic Ocean, Prog. Oceanogr., 26, 1–73, https://doi.org/10.1016/0079-6611(91)90006-8, 1991.

Piña-Ochoa, E., Høgslund, S., Geslin, E., Cedhagen, T., Revsbech, N. P., Nielsen, L. P., Schweizer, M., Jorissen, F., Rysgaard, S., and Risgaard-Petersen, N.: Widespread occurrence of nitrate storage and denitrification among Foraminifera and Gromiida, P. Natl. Acad. Sci. USA, 107, 1148–1153, https://doi.org/10.1073/pnas.0908440107, 2010.

Rashid, H. and Boyle, E. A.: Mixed-layer deepening during Heinrich events: A multi-planktonic foraminiferal δ18O approach, Science, 318, 439–441, https://doi.org/10.1126/science.1146138, 2007.

Ravelo, A. and Fairbanks, R.: Oxygen isotopic composition of multiple species of planktonic foraminifera: Recorders of the modern photic zone temperature gradient, Paleoceanography, 7, 815–831, 1992.

Rebotim, A., Voelker, A. H. L., Jonkers, L., Waniek, J. J., Meggers, H., Schiebel, R., Fraile, I., Schulz, M., and Kucera, M.: Factors controlling the depth habitat of planktonic foraminifera in the subtropical eastern North Atlantic, Biogeosciences, 14, 827–859, https://doi.org/10.5194/bg-14-827-2017, 2017.

Reid, J. L., Nowlin Jr, W. D., and Patzert, W. C.: On the characteristics and circulation of the southwestern Atlantic Ocean, J. Phys. Oceanogr., 7, 62–91, https://doi.org/10.1175/1520-0485(1977)007<0062:OTCACO>2.0.CO;2, 1977.

Ren, H., Sigman, D., Meckler, A., Plessen, B., Robinson, R., Rosenthal, Y., and Haug, G.: Foraminiferal isotope evidence of reduced nitrogen fixation in the ice age Atlantic Ocean, Science, 323, 244–248, https://doi.org/10.1126/science.1165787, 2009.

Ren, H., Sigman, D. M., Chen, M. T., and Kao, S. J.: Elevated foraminifera-bound nitrogen isotopic composition during the last ice age in the South China Sea and its global and regional implications, Global Biogeochem. Cycles, 26, GB1031, https://doi.org/10.1029/2010GB004020, 2012a.

Ren, H., Sigman, D. M., Thunell, R. C., and Prokopenko, M. G.: Nitrogen isotopic composition of planktonic foraminifera from the modern ocean and recent sediments, Limnol. Oceanogr., 57, 1011–1024, https://doi.org/10.4319/lo.2012.57.4.1011, 2012b.

Ren, H., Studer, A. S., Serno, S., Sigman, D. M., Winckler, G., Anderson, R. F., Oleynik, S., Gersonde, R., and Haug, G. H.: Glacial-to-interglacial changes in nitrate supply and consumption in the subarctic North Pacific from microfossil-bound N isotopes at two trophic levels, Paleoceanography, 30, 1217–1232, https://doi.org/10.1002/2014PA002765, 2015.

Ren, H., Sigman, D. M., Martínez-García, A., Anderson, R. F., Chen, M.-T., Ravelo, A. C., Straub, M., Wong, G. T., and Haug, G. H.: Impact of glacial/interglacial sea level change on the ocean nitrogen cycle, P. Natl. Acad. Sci. USA, 114, E6759–E6766, https://doi.org/10.1073/pnas.1701315114, 2017.

Repschläger, J., Auderset, A., Blanz, T., Bremer, K., Böttner, C., Eich, C., Kausch, T., Keigwin, L. D., Keul, N., and Kiefer, J.: North Atlantic Subtropical Gyre Azores Front (NASGAF), Cruise No. MSM58/1, September 10, 2016-October 7, 2016, Reykjavik (Iceland)-Ponta Delgada (Azores, Portugal), Gutachterpanel Forschungsschiffe, https://doi.org/10.2312/cr_msm58_1, 2018.

Reynolds, C. E., Richey, J. N., Fehrenbacher, J. S., Rosenheim, B. E., and Spero, H. J.: Environmental controls on the geochemistry of Globorotalia truncatulinoides in the Gulf of Mexico: Implications for paleoceanographic reconstructions, Marine Micropaleontol., 142, 92–104, https://doi.org/10.1016/j.marmicro.2018.05.006, 2018.

Robinson, R. S., Brunelle, B. G., and Sigman, D. M.: Revisiting nutrient utilization in the glacial Antarctic: Evidence from a new method for diatom-bound N isotopic analysis, Paleoceanography, 19, PA3001, https://doi.org/10.1029/2003PA000996, 2004.

Robinson, R. S., Kienast, M., Luiza Albuquerque, A., Altabet, M., Contreras, S., De Pol Holz, R., Dubois, N., Francois, R., Galbraith, E., and Hsu, T. C.: A review of nitrogen isotopic alteration in marine sediments, Paleoceanography, 27, PA4203, https://doi.org/10.1029/2012PA002321, 2012.

Salmon, K. H., Anand, P., Sexton, P. F., and Conte, M.: Upper ocean mixing controls the seasonality of planktonic foraminifer fluxes and associated strength of the carbonate pump in the oligotrophic North Atlantic, Biogeosciences, 12, 223–235, https://doi.org/10.5194/bg-12-223-2015, 2015.

Sarmiento, J. L. and Gruber, N.: Ocean Biogeochemical Dynamics, Princeton University Press, https://doi.org/10.1515/9781400849079, 2006.

Schiebel, R. and Hemleben, C.: Planktic foraminifers in the modern ocean, Springer, https://doi.org/10.1007/978-3-662-50297-6, 2017.

Schiebel, R., Hiller, B., and Hemleben, C.: Impacts of storms on recent planktic foraminiferal test production and CaCO3 flux in the North Atlantic at 47° N, 20° W (JGOFS), Marine Micropaleontol., 26, 115–129, https://doi.org/10.1016/0377-8398(95)00035-6, 1995.

Schiebel, R., Waniek, J., Bork, M., and Hemleben, C.: Planktic foraminiferal production stimulated by chlorophyll redistribution and entrainment of nutrients, Deep-Sea Res. Pt. I, 48, 721–740, https://doi.org/10.1016/S0967-0637(00)00065-0, 2001.

Schiebel, R., Schmuker, B., Alves, M., and Hemleben, C.: Tracking the Recent and late Pleistocene Azores front by the distribution of planktic foraminifers, J. Marine Syst., 37, 213–227, https://doi.org/10.1016/S0924-7963(02)00203-8, 2002.

Schiebel, R., Smart, S. M., Jentzen, A., Jonkers, L., Morard, R., Meilland, J., Michel, E., Coxall, H. K., Hull, P. M., and de Garidel-Thoron, T.: Advances in planktonic foraminifer research: New perspectives for paleoceanography, Revue de Micropaleontologie, 61, 113–138, https://doi.org/10.1016/j.revmic.2018.10.001, 2018.

Schlitzer, R.: Data analysis and visualization with Ocean Data View, CMOS Bulletin SCMO, 43, 9–13, 2015.

Schmid, C., Siedler, G., and Zenk, W.: Dynamics of intermediate water circulation in the subtropical South Atlantic, J. Phys. Oceanogr., 30, 3191–3211, https://doi.org/10.1175/1520-0485(2000)030<3191:DOIWCI>2.0.CO;2, 2000.

Schmidt, D. N., Renaud, S., Bollmann, J., Schiebel, R., and Thierstein, H. R.: Size distribution of Holocene planktic foraminifer assemblages: biogeography, ecology and adaptation, Marine Micropaleontol., 50, 319–338, https://doi.org/10.1016/S0377-8398(03)00098-7, 2004.

Schmitz Jr., W. J. and McCartney, M. S.: On the North Atlantic Circulation, Rev. Geophys., 31, 29–49, https://doi.org/10.1029/92RG02583, 1993.

Schubert, C. J. and Calvert, S. E.: Nitrogen and carbon isotopic composition of marine and terrestrial organic matter in Arctic Ocean sediments:: implications for nutrient utilization and organic matter composition, Deep-Sea Res. Pt. I, 48, 789–810, https://doi.org/10.1016/S0967-0637(00)00069-8, 2001.

Shaw, J. O., D'haenens, S., Thomas, E., Norris, R. D., Lyman, J. A., Bornemann, A., and Hull, P. M.: Photosymbiosis in planktonic foraminifera across the Paleocene–Eocene thermal maximum, Paleobiology, 47, 632–647, https://doi.org/10.1017/pab.2021.7, 2021.

Siccha, M., Morard, R., and Kucera, M.: Processed multinet CTD data from METEOR cruise M124, PANGAEA [data set], https://doi.org/10.1594/PANGAEA.895426, 2018.

Sigman, D., Casciotti, K., Andreani, M., Barford, C., Galanter, M., and Böhlke, J.: A bacterial method for the nitrogen isotopic analysis of nitrate in seawater and freshwater, Anal. Chem., 73, 4145–4153, https://doi.org/10.1021/ac010088e, 2001.

Sigman, D. M., Altabet, M. A., Francois, R., McCorkle, D. C., and Gaillard, J. F.: The isotopic composition of diatom-bound nitrogen in Southern Ocean sediments, Paleoceanography, 14, 118–134, https://doi.org/10.1029/1998PA900018, 1999.

Sigman, D. M., Altabet, M., McCorkle, D., Francois, R., and Fischer, G.: The δ15N of nitrate in the Southern Ocean: Nitrogen cycling and circulation in the ocean interior, J. Geophys. Res.-Oceans, 105, 19599–19614, https://doi.org/10.1029/2000JC000265, 2000.

Silfer, J., Engel, M., and Macko, S.: Kinetic fractionation of stable carbon and nitrogen isotopes during peptide bond hydrolysis: experimental evidence and geochemical implications, Chem. Geol.: Isotope Geoscience section, 101, 211–221, https://doi.org/10.1016/0009-2541(92)90003-N, 1992.

Smart, S. M., Fawcett, S. E., Thomalla, S. J., Weigand, M. A., Reason, C. J., and Sigman, D. M.: Isotopic evidence for nitrification in the Antarctic winter mixed layer, Global Biogeochem. Cycles, 29, 427–445, https://doi.org/10.1002/2014GB005013, 2015.

Smart, S. M., Ren, H., Fawcett, S. E., Schiebel, R., Conte, M., Rafter, P. A., Ellis, K. K., Weigand, M. A., Oleynik, S., Haug, G. H., and Sigman, D. M.: Ground-truthing the planktic foraminifer-bound nitrogen isotope paleo-proxy in the Sargasso Sea, Geochim. Cosmochim. Ac., 235, 463–482, https://doi.org/10.1016/j.gca.2018.05.023, 2018.

Smart, S. M., Fawcett, S. E., Ren, H., Schiebel, R., Tompkins, E. M., Martínez-García, A., Stirnimann, L., Roychoudhury, A., Haug, G. H., and Sigman, D. M.: The nitrogen isotopic composition of tissue and shell-bound organic matter of planktic foraminifera in Southern Ocean surface waters, Geochem. Geophys. Geosyst., 21, e2019GC008440, https://doi.org/10.1029/2019GC008440, 2020.

Spero, H. and Williams, D.: Opening the carbon isotope "vital effect" black box 1. Seasonal temperatures in the euphotic zone, Paleoceanography, 4, 593–601, 1989.

Spero, H. J. and DeNiro, M. J.: The influence of symbiont photosynthesis on the δ18O and δ13C values of planktonic foraminiferal shell calcite, Symbiosis, 4, 213–228, 1987.

Spero, H. J. and Lea, D. W.: Experimental determination of stable isotope variability in Globigerina bulloides: implications for paleoceanographic reconstructions, Marine Micropaleontol., 28, 231–246, https://doi.org/10.1016/0377-8398(96)00003-5, 1996.

Spero, H. J., Lerche, I., and Williams, D. F.: Opening the carbon isotope "vital effect" black box, 2, Quantitative model for interpreting foraminiferal carbon isotope data, Paleoceanography, 6, 639–655, https://doi.org/10.1029/91PA02022, 1991.

Spero, H. J., Bijma, J., Lea, D. W., and Bemis, B. E.: Effect of seawater carbonate concentration on foraminiferal carbon and oxygen isotopes, Nature, 390, 497–500, https://doi.org/10.1038/37333, 1997.

Spindler, M., Hemleben, C., Salomons, J., and Smit, L.: Feeding behavior of some planktonic foraminifers in laboratory cultures, J. Foramin. Res., 14, 237–249, https://doi.org/10.2113/gsjfr.14.4.237, 1984.

Steinberg, D. K., Carlson, C. A., Bates, N. R., Johnson, R. J., Michaels, A. F., and Knap, A. H.: Overview of the US JGOFS Bermuda Atlantic Time-series Study (BATS): a decade-scale look at ocean biology and biogeochemistry, Deep-Sea Res. Pt. II, 48, 1405–1447, https://doi.org/10.1016/S0967-0645(00)00148-X, 2001.

Stramma, L.: Geostrophic transport of the South Equatorial Current in the Atlantic, J. Marine Res., 49, 281–294, 1991.

Straub, M., Sigman, D. M., Ren, H., Martínez-García, A., Meckler, A. N., Hain, M. P., and Haug, G. H.: Changes in North Atlantic nitrogen fixation controlled by ocean circulation, Nature, 501, 200, https://doi.org/10.1038/nature12397, 2013.

Takagi, H., Kimoto, K., Fujiki, T., Kurasawa, A., Moriya, K., and Hirano, H.: Ontogenetic dynamics of photosymbiosis in cultured planktic foraminifers revealed by fast repetition rate fluorometry, Marine Micropaleontol., 122, 44–52, https://doi.org/10.1016/j.marmicro.2015.10.003, 2016.

Takagi, H., Kimoto, K., Fujiki, T., Saito, H., Schmidt, C., Kucera, M., and Moriya, K.: Characterizing photosymbiosis in modern planktonic foraminifera, Biogeosciences, 16, 3377–3396, https://doi.org/10.5194/bg-16-3377-2019, 2019.

Takagi, H., Kimoto, K., and Fujiki, T.: Photosynthetic carbon assimilation and electron transport rates in two symbiont-bearing planktonic foraminifera, Front. Marine Sci., 9, 803354, https://doi.org/10.3389/fmars.2022.803354, 2022.

Uhle, M. E., Macko, S. A., Spero, H. J., Lea, D. W., Ruddiman, W. F., and Engel, M. H.: The fate of nitrogen in the Orbulina universa foraminifera-symbiont system determined by nitrogen isotope analyses of shell-bound organic matter, Limnol. Oceanogr., 44, 1968–1977, https://doi.org/10.4319/lo.1999.44.8.1968, 1999.

Wang, X. T., Prokopenko, M. G., Sigman, D. M., Adkins, J. F., Robinson, L. F., Ren, H., Oleynik, S., Williams, B., and Haug, G. H.: Isotopic composition of carbonate-bound organic nitrogen in deep-sea scleractinian corals: A new window into past biogeochemical change, Earth Planet. Sc. Lett., 400, 243–250, https://doi.org/10.1016/j.epsl.2014.05.048, 2014.

Wang, X., Sigman, D. M., Cohen, A., Sinclair, D., Sherrell, R., Weigand, M., Erler, D. V., and Ren, H.: Isotopic composition of skeleton-bound organic nitrogen in reef-building symbiotic corals: A new method and proxy evaluation at Bermuda, Geochim. Cosmochim. Ac., 148, 179–190, https://doi.org/10.1016/j.gca.2014.09.017, 2015.

Wang, X. T., Wang, Y., Auderset, A., Sigman, D. M., Ren, H., Martínez-García, A., Haug, G. H., Su, Z., Zhang, Y. G., and Rasmussen, B.: Oceanic nutrient rise and the late Miocene inception of Pacific oxygen-deficient zones, P. Natl. Acad. Sci. USA, 119, e2204986119, https://doi.org/10.1073/pnas.2204986119, 2022.

Wefer, G., Berger, W. H., Siedler, G., Webb, D. J., and Reid, J.: On the circulation of the South Atlantic Ocean, The South Atlantic: present and past circulation, 13–44, https://doi.org/10.1007/978-3-642-80353-6_2, 1996.

Weigand, M. A., Foriel, J., Barnett, B., Oleynik, S., and Sigman, D. M.: Updates to instrumentation and protocols for isotopic analysis of nitrate by the denitrifier method, Rapid Commun. Mass Sp., 30, 1365–1383, https://doi.org/10.1002/rcm.7570, 2016.

Yoshikawa, C., Makabe, A., Shiozaki, T., Toyoda, S., Yoshida, O., Furuya, K., and Yoshida, N.: Nitrogen isotope ratios of nitrate and N* anomalies in the subtropical South Pacific, Geochem. Geophys. Geosyst., 16, 1439–1448, https://doi.org/10.1002/2014GC005678, 2015.

Yoshikawa, C., Makabe, A., Matsui, Y., Nunoura, T., and Ohkouchi, N.: Nitrate isotope distribution in the subarctic and subtropical North Pacific, Geochem. Geophys. Geosyst., 19, 2212–2224, https://doi.org/10.1029/2018GC007528, 2018.